Global and Planetary Change 222 (2023) 104074

Contents lists available at ScienceDirect

Global and Planetary Change

journal homepage: www.elsevier.com/locate/gloplacha

Carbon cycle during the late Aptian–early Albian OAE 1b: A focus on the Kilian–Paquier levels interval

Stéphane Bodin [a,*], Mickaël Charpentier [a], Clemens V. Ullmann [b], Arka Rudra [a], Hamed Sanei [a]

[a] Department for Geoscience, Aarhus University, Hoegh-Guldbergs Gade 2, 8000 Aarhus C, Denmark
[b] Camborne School of Mines, University of Exeter, Penryn Campus, Penryn, Cornwall TR10 9FE, UK

ARTICLE INFO

Editor Name: Dr. Alan Haywood

Keywords:
Cretaceous
Carbon isotope record
Monsoon-driven system
South-East France Basin
Blue Marl Formation

ABSTRACT

The Oceanic Anoxic Event (OAE) 1b took place over a protracted time interval during the Aptian/Albian boundary interval, at the dawn of the mid-Cretaceous climatic optimum. OAE 1b is characterized by the occurrence of several sub-events recorded by organic matter-rich levels, which can be traced on regional-to-global scale. Previous studies have highlighted that the climax of the event occurred around the Kilian – Paquier interval, with this latter sub-event being the most extended and pronounced stratigraphic interval. Numerous studies on OAE 1b have however only focused on high-precision investigations of the Kilian and/or Paquier levels, leaving vast uncertainties about the environmental changes and their drivers during the entire OAE 1b, and hence also on the mechanisms leading to the formation of the sub-events themselves. In this study, we have performed a high-resolution multi-proxy analysis of the Briers section, a well-exposed section in the Blue Marls Formation of the SE France Vocontian Basin, continuously covering the Kilian – Paquier interval. Pyrolysis analyses show that most of the organic matter in this section is immature and of continental origin, averaging 1.5% TOC. The Kilian and Paquier levels are characterized by higher TOC values and a substantial increase in the amount of marine organic matter. Comparing TOC values with changes in Al or Ti concentration (proxies for continental weathering) and Hydrogen index (HI values, tracer for the type of organic matter) reveals that the background long-term change in TOC is linked to change in the continental organic matter delivery to the Vocontian Basin tied to changes in continental weathering rates. Sporadic increases in TOC values associated with the Kilian, HN 8, and Paquier levels, are most likely the result of short-lived events of increased marine primary productivity and organic matter preservation superimposed on the background influx of continental organic matter. A high-resolution bulk organic matter carbon isotope record shows that, apart from the Paquier level, all the fluctuations observed in the carbonate carbon isotope ratios are also mirrored in the organic matter record, although with higher amplitudes. This discrepancy in amplitude can be resolved by correcting the bulk organic matter carbon isotope record for fluctuations in the type of organic matter, demonstrating that both oceanic and atmospheric reservoirs were affected by similar carbon isotope fluctuations, which were hence of global extent. The abnormal bulk organic matter carbon isotope record of the Paquier level further confirms the large geographical expansion of unusual organic matter production and/or accumulation during this peculiar event. Overall, this study suggests that Milankovitch-paced (long eccentricity) changes in monsoonal activity and their effect on the accumulation of organic matter in continental wetlands best explains the rhythmic change in the global carbon isotope record across the OAE 1b interval.

1. Introduction

Deviating from the norm of Greenhouse climate, the Cretaceous Period was punctuated by numerous episodes of climatic and environmental perturbations, either toward super-greenhouse states (so-called hyperthermal events, or Oceanic Anoxic Events – OAEs; Jenkyns, 2010), or toward transient cooling episodes leading to the intermittent growth of ice caps at the pole (Bodin et al., 2015; O'Brien et al., 2017; Alley et al., 2020). The Aptian/Albian boundary interval is here of great interest as it encompasses the transition from the late Aptian cold climate interlude (likely one of the coldest time intervals of the Cretaceous; e.g., Bodin et al., 2015; O'Brien et al., 2017) to the early Albian OAE 1b,

* Corresponding author.
E-mail address: stephane.bodin@geo.au.dk (S. Bodin).

https://doi.org/10.1016/j.gloplacha.2023.104074
Received 2 August 2022; Received in revised form 5 February 2023; Accepted 16 February 2023
Available online 20 February 2023

harbinger of the mid-Cretaceous warmth (Bottini and Erba, 2018; Huber et al., 2018). Understanding the modality and causes of this pronounced climatic transition offers thus a valuable perspective on the Cretaceous Greenhouse climate.

Compared to other Mesozoic OAEs, less is known about the exact causes and unfolding of OAE 1b. Fuelled by the detailed litho- and biostratigraphic work of Bréhéret (1997) on the Blue Marls Formation in SE France, the study of OAE 1b was ramped up by the high-resolution carbon isotopes record established by Herrle et al. (2004), which has proven instrumental for chemostratigraphic purposes and therefore better correlation of the OAE 1b sub-events across different basins (e.g., Coccioni et al., 2014; Herrle et al., 2015; Navarro-Ramirez et al., 2015). Despite this, it is yet not clear whether the bulk carbonate $\delta^{13}C$ record established by Herrle et al. (2004) accounts only for changes in oceanic carbon cycle, or if it accounts also for atmospheric, and hence global change in carbon cycle. In the latter case, high-resolution correlations between marine and terrestrial records would become possible. This uncertainty is due to the fact that there is currently no high-resolution $\delta^{13}C$ record established in continental organic matter across the Aptian/Albian boundary interval, and consequently, understanding of the cause of the carbon isotope fluctuations during the OAE 1b interval is presently limited.

In order to better understand the extent and cause of the carbon cycle fluctuations during the OAE 1b, we present a high-resolution dataset covering the climax part of this time interval, which encompasses the Kilian and the Paquier levels. For this purpose, a well-exposed and extended section in the Vocontian Basin (SE France) was studied: Les Briers. This new dataset is made of organic matter pyrolysis analyses, stable carbon isotope ratios from both bulk carbonate and organic matter, and element concentration analysis. With this dataset, we aim to: i) reconstruct the evolution of the amount and type of organic matter during this critical time interval, ii) understand the factors (local vs. global) having controlled their deposition, and iii) their influence on the bulk organic matter stable carbon isotope ($\delta^{13}C_{org}$) record. By correcting the $\delta^{13}C_{org}$ record for changes in organic matter type (continental vs. marine), the marine bulk carbonate stable carbon isotope ($\delta^{13}C_{carb}$) can be compared to a calculated continental $\delta^{13}C$ signal reflecting change in atmospheric, and hence global carbon cycle. This will allow to propose a conceptual model of the carbon cycle changes during the OAE 1b cluster.

2. Geological setting

2.1. The Briers section

The Briers section is situated is SE France, close to the town of Saint-André-les-Alpes (Fig. 1). It is located on the north-eastern side of the Castillon Lake, on the territory of the ancient municipality of Méouilles. The GPS coordinates of the base of the section are: N43.95273, E6.53041 (WGS84).

The studied section belongs to the South-East France Basin. It was deposited during the Vocontian period of this basin, which saw the development of a relatively narrow deep-water domain during the latest Hauterivian – Cenomanian compared to its more extended phase during previous Mesozoic time (Arnaud, 2005). The Vocontian Basin was fringed to the West by the carbonate and siliciclastic platforms that are the sedimentary cover of the Massif Central, to the South by the Provence platform, and to the north by an extensive carbonate platform now preserved in the Jura Mountain and the Helvetic nappes. To the East, it was open to the Tethyan ocean, presently outcropping in the internal zones of the Alps (Fig. 1A).

During the late early Aptian – early Cenomanian, thick marl-dominated deposition took place in the centre of the basin. They are known as the "Formation des Marnes Bleues", i.e. the Blue Marls Formation in English. The basin centre was surrounded by siliciclastic-dominated shallow-water areas (Bréhéret, 1997). A robust lithostratigraphic and biostratigraphic scheme has been established for the Blue Marls Formation based on ammonite and foraminifera (e.g., Bréhéret, 1997; Herrle et al., 2004; Joly and Delamette, 2008; Gale et al., 2011). This is complemented by a high-resolution $\delta^{13}C$ chemostratigraphic reference curve (Herrle et al., 2004) allowing to trace each individual levels within the Blue Marls Formation with high confidence across all this basin and beyond (Fig. 2). This basin also hosts several Jurassic and Cretaceous GSSPs, out of which the base of the Albian stage is of most interest here. The base of the Albian is defined as the first occurrence of

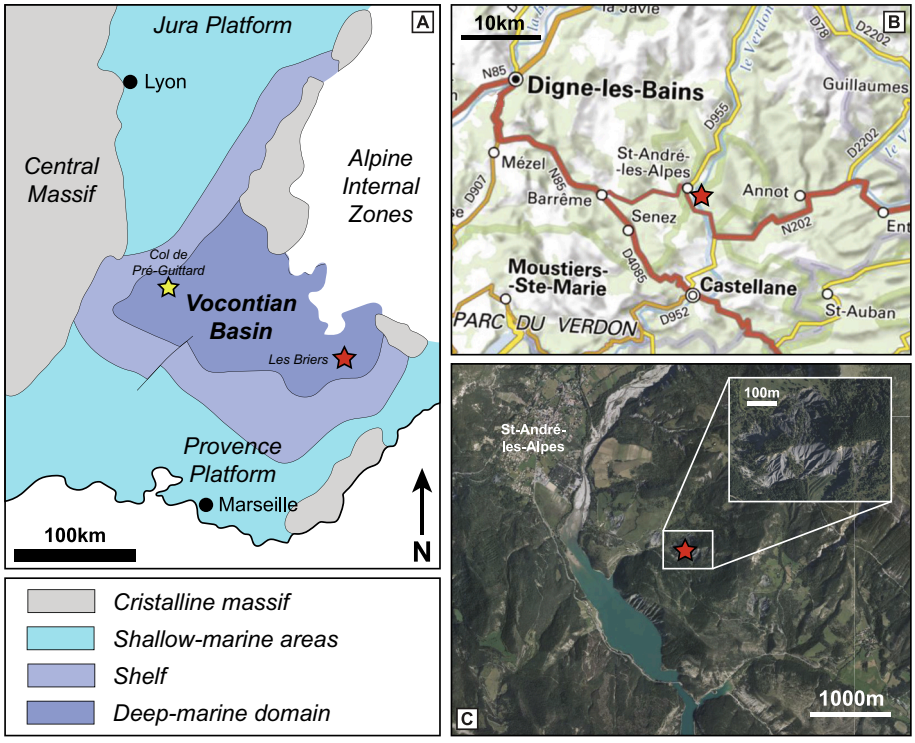

Fig. 1. Geographic and geologic setting of the Briers section (red star). A. Late Early Cretaceous paleogeographic map of SE France (Vocontian) Basin (modified after Ferry, 2017). The yellow star indicates the position of the Col de Pré-Guittard section, which hosts the GSSP for the base of the Albian stage (Kennedy et al., 2017). B. Geographic map of the Digne-les-Bains – Castellane area, SE France (modified from geoportail.gouv.fr). The Briers section is situated next to Saint-André-les-Alpes, in the ancient municipality of Meouilles. C. Aerial picture of the south-eastern vicinity of Saint-André-les-Alpes (modified from geoportail.gouv.fr), showing the precise location of the Briers section. (For interpretation of the references to colour in this figure legend, the reader is referred to the web version of this article.)

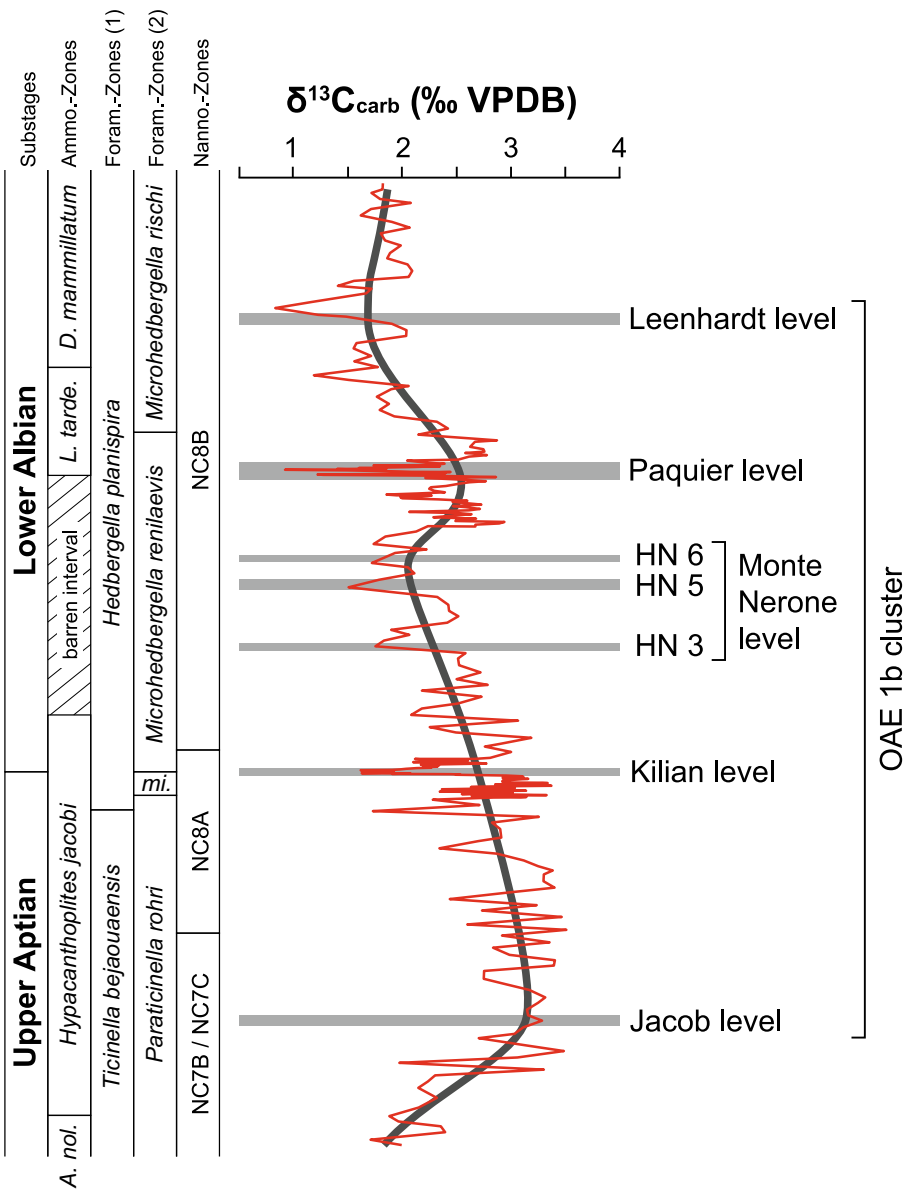

Fig. 2. Position of the OAE 1b sub-events compared to biostratigraphic and chemostratigraphic markers in the Vocontian Basin. Reference high-resolution $\delta^{13}C$ curve for the OAE 1b cluster derived from bulk carbonate (Herrle et al., 2004). The dark grey line underlines the long-term trend. Foraminifera zonation (1) is after Herrle et al. (2004), foraminifera zonation (2) is after Kennedy et al. (2017). Abbreviation; mi, *Microhedbergella miniglobularis*; L. tarde, *Leymeriella tardefurcata*; A. nol., *Acanthohoplites nolani*; D. mammillatum, *Douvilleiceras mammillatum*.

the planktonic foraminifera *Microhedbergella renilaevis*, conveniently situated within the Kilian level, 40 cm above its base, in the section of the Col de Pré-Guittard (Kennedy et al., 2017).

A detailed lithostratigraphic description of the Briers section can be found in Bréhéret (1997) (see also Wang et al., 2022). This section is a detailed upper part of the Meouilles section that covers the Aptian–early Albian interval. A notable condensed level occurs in the lower upper Aptian and corresponds to the Nolan-Fromaget interval observed in other parts of the basin. Importantly, this condensed interval also includes the Jacob level, which is hence absent in this section. The here-studied Briers section starts above this condensed interval. It encompasses 89 m of the Blue Marls Formation (Fig. 3), including the Kilian and Paquier levels, and numerous other black-coloured levels named HN 1 to HN 13 (for "Horizon noir"), following the classification of Bréhéret (1997). The studied interval in the Briers section encompasses the *Hypacanthoplites jacobi* to *Leymeriella tardefurcata* ammonite zones (Fig. 3; Bréhéret, 1997; Joly and Delamette, 2008). The Paquier level is particularly well visible in the field as it corresponds to a less recessive interval of black "paper-shale" deposits (Fig. 3B).

2.2. Definition of OAE 1b

The concept of Oceanic Anoxic Events was pioneered by Schlanger and Jenkyns (1976) who noted the global development of organic-rich sediments in pelagic setting during the Aptian-Albian and the Cenomanian-Turonian; OAE 1 and OAE 2, respectively. Over the succeeding 20 years, improved chronostratigraphic resolution led to the further subdivision of OAE 1 into several distinct events, out of which OAE 1a (early Aptian) and OAE 1b (Aptian–Albian transition) are the best documented ones with an unequivocally global reach (Arthur et al., 1990; see also Jenkyns, 2010). Contrary to OAE 1a, which is associated with a unique organic matter-rich level in most of deep-water records (e.g., Livello Selli in Italy – Coccioni et al., 1992; Niveau Goguel in France – Bréhéret, 1997), the more complex lithostratigraphic expression of the organic-matter enrichment around the Aptian–Albian transition has led to discrepancy among authors about the definition of OAE 1b. Hence, in the Vocontian Basin in SE France, a reference region for the Aptian–Albian transition, numerous organic matter-rich levels are observed in this stratigraphic interval (Bréhéret, 1997; Fig. 2). They are named HN followed by a number according to their relative stratigraphic position. Out of those, four levels of peculiar importance have

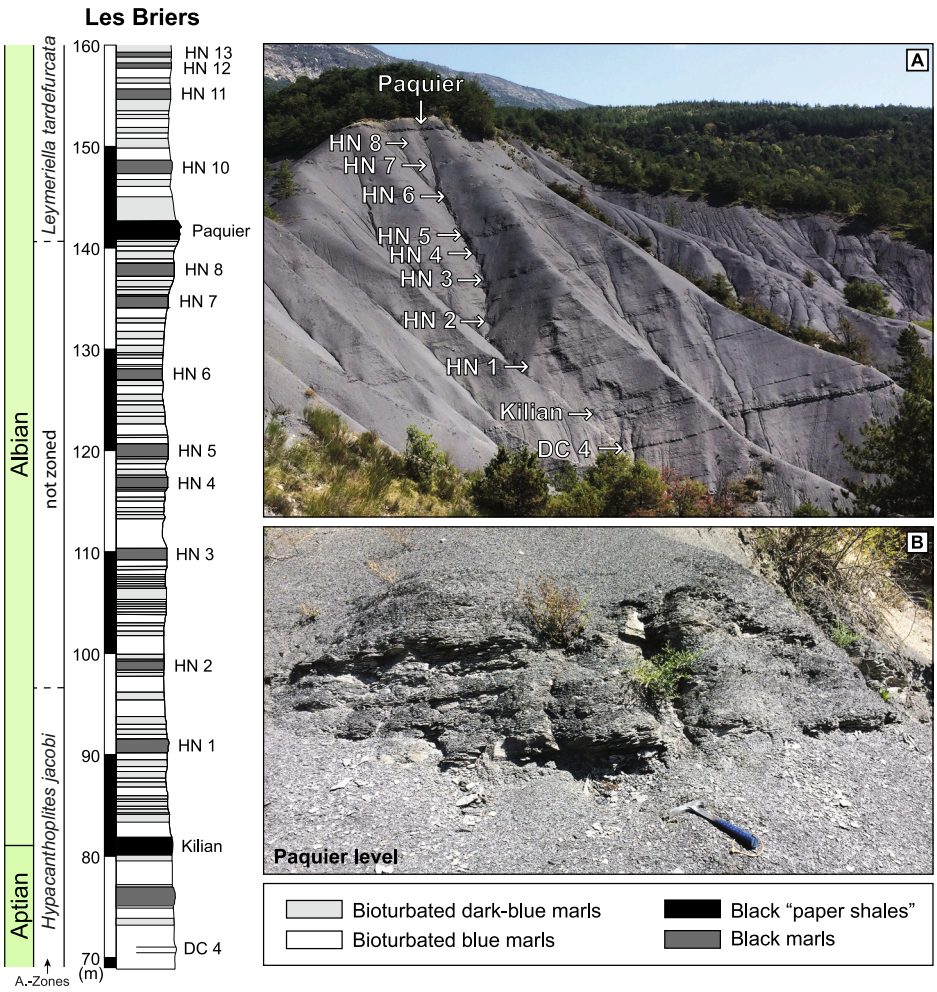

Fig. 3. Measured lithostratigraphic log of the Briers section, indicating the position of all the remarkable horizons (DC: "délit calcaire"; HN: "horizon noir"). Ammonite biostratigraphy after Bréhéret (1997) and Joly and Delamette (2008). A. Field picture of the Briers outcrop. B. Close-up view on the Paquier level (hammer for scale is 28 cm long).

been given a more specific name. From the lowest to the highest, these are: the Jacob level, the Kilian level, the Paquier level, and the Leenhardt level (Fig. 2; Bréhéret, 1997). The equivalents of these four levels are observed in several basins across the globe (Fig. 4), with the Kilian and Paquier levels being the most commonly observed and prominent of them (Bralower et al., 1999; Trabucho Alexandre et al., 2011; Peybernes et al., 2013; Millán et al., 2014; Herrle et al., 2015; Navarro-Ramirez et al., 2015; Sabatino et al., 2015). In Italy, another peculiar level of organic matter enrichment is observed between the Kilian and Paquier levels: The Monte Nerone level (Coccioni et al., 2014). It is correlated to the stratigraphic interval covering the HN3 – HN6 levels in France based on high resolution biostratigraphy and carbon isotope chemostratigraphy (Coccioni et al., 2014; Fig. 2).

Together, the stratigraphic interval covered by these five organic matter-rich levels constitutes the OAE 1b cluster according to some authors (e.g., Leckie et al., 2002; Coccioni et al., 2014; Sabatino et al., 2015), while other consider only the Paquier level (and its equivalent throughout the world) as the lithological expression of OAE 1b (e.g., Bralower et al., 1993; Herrle et al., 2004; Jenkyns, 2010). This is based on the rationale that the Paquier level is the best expressed and globally traceable organic matter-rich layer in the Aptian/Albian boundary interval. This latter concept hence follows the original description of OAE 1b by Arthur et al. (1990). It has however proven to be misleading due to the difficulty of attributing organic matter-rich levels from the Aptian/Albian boundary interval to a specific reference level from the Vocontian Basin. In this regard, the case of the organic matter-rich level in DSDP hole 545 is very illustrative. Attributed originally to the Paquier level (Bralower et al., 1993; Herrle et al., 2004), it is now correlated to the Kilian level following a detailed planktonic foraminifera study (Huber and Leckie, 2011), complemented by lithological and geochemical evidences (Trabucho Alexandre et al., 2011). As a consequence, the initial rationale of equalling OAE 1b and the Paquier level, based on the assumption that this latter level was the only organic matter-rich level of the Aptian/Albian boundary interval present in the Atlantic Ocean (e.g., Arthur et al., 1990), is flawed. Similar difficulties have also been encountered in Italy where, for instance, the Monte Nerone level was previously correlated either to the Kilian level or the Paquier level (e.g., Erbacher, 1994; Leckie et al., 2002; Trabucho Alexandre et al., 2011; Petrizzo et al., 2012), before being finally recognized as a fifth organic matter-rich level comprised between the Kilian and Paquier levels (Coccioni et al., 2014). A recent thallium isotope study in the Briers section (Wang et al., 2022) nevertheless confirms that substantial global marine deoxygenation only occurred during the unfolding of the Paquier level (and to a lesser extend the preceding HN 8 level), giving credit to the original assumption of Arthur et al. (1990). Further complications also arose from the absence of a consensus about the definition of the Aptian/Albian boundary until its recent ratification (Kennedy et al., 2017), which can lead to confusion when navigating through older literature, especially in the absence of a precise biostratigraphic or chemostratigraphic framework.

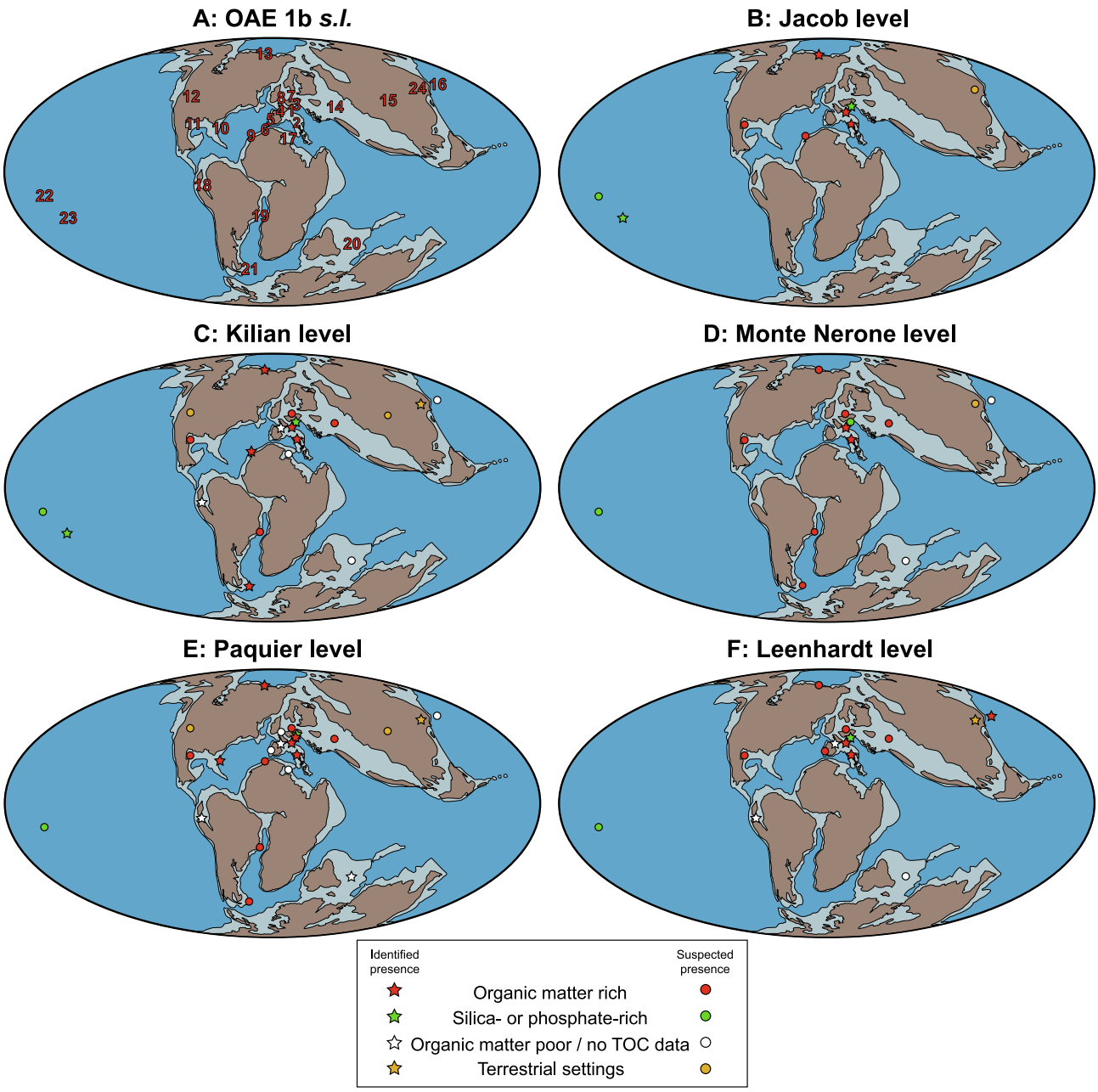

Fig. 4. Palaeogeographic distribution of OAE 1b records. Early Albian paleogeographic map modified after Scotese (2016) A. Localities spanning the Aptian-Albian transition where lithological, geochemical, or paleontological evidences relates to the OAE 1b sensu *lato*. 1. Vocontian Basin, France (Bréhéret and Crumière, 1989; Herrle et al., 2004). 2. Umbria-Marche Basin, Italy (Coccioni et al., 2014). 3. Helvetic shelf and Briançonnais Domain, Switzerland (Strasser et al., 2001; Föllmi et al., 2007). 4. Basque–Cantabrian Basin, Spain (Millán et al., 2014). 5. Algarve Basin, Portugal (Heimhofer et al., 2003). 6. Essaouira-Agadir Basin, Morocco (Peybernes et al., 2013). 7. Lower Saxony Basin, Germany (Mutterlose et al., 2003). 8. Wessex Basin, England (Gröcke, 2002). 9. DSDP site 545, Mazagan Plateau, eastern Proto-North Atlantic (Wagner et al., 2008; Huber and Leckie, 2011; McAnena et al., 2013). 10. ODP site 1049, Blake Plateau, western Proto-North Atlantic (Erbacher et al., 2001; Huber and Leckie, 2011). 11. Northern Cordillera, Mexico, and Comanche Platform, Texas (Bralower et al., 1999; Phelps et al., 2015). 12. Western Interior, Utah (Ludvigson et al., 2015). 13. Axel Heiberg Island, Canada (Herrle et al., 2015). 14. Northeastern peri-Tethys, Caucasus region (Gavrilov et al., 2019). 15. Yujingzi Basin, northwest China (Suarez et al., 2018). 16. Hokkaido, Japan (Ando and Kakegawa, 2007). 17. Tunisian Platform, Tunisia (Ben Chaabane et al., 2019). 18. Western Platform, Peru (Navarro-Ramirez et al., 2015). 19. Central Proto-South Atlantic, Brazil (Caetano-Filho et al., 2017). 20. Southern Tibet, China (Li et al., 2016). 21. DSDP Site 511, Falkland Plateau, southern South Atlantic (Huber and Leckie, 2011; Huber et al., 2018; Matsumoto et al., 2023). 22. ODP sites 1207 and 1213, Shatsky Rise, northwest Pacific (Robinson et al., 2004). 23. DSDP site 463, Resolution Guyot, Mid-Pacific Mountains (Price, 2003; Matsumoto et al., 2020). 24. Fuxin Basin, Northeast China (Xu et al., 2022). B—F. For each OAE 1b sub-levels, map showing the localities where their presence can be identified (star) or suspected (circle), as well as the type of lithological expression.

Taking these difficulties into account, it is thus interesting to note that our knowledge of the OAE 1b rests on interpretations that are in some cases based on imprecise or wrong lithostratigraphic attribution and correlation, as well as on the confusion between the OAE 1b cluster and the Paquier level. In this manuscript, we follow the more versatile definition of OAE 1b as an extended stratigraphic interval regrouping the Jacob, Kilian, Monte Nerone, Paquier and Leenhardt levels (Sabatino et al., 2015). To avoid confusion, we refer to this ensemble as the OAE 1b cluster (Fig. 2), and name the different sub-events according to the name of the organic matter-rich levels in SE France (for the Jacob, Kilian,

Paquier and Leenhardt levels) and in Italy (for the Monte Nerone Level).

3. Methods

3.1. Field sampling

The Briers section was sampled along one of the crests separating the numerous talwegs present in the Blue Marls Formation (see Wang et al., 2022). During the sampling, surface sediments were dug out to reveal fresh, unaltered material. A total of 213 samples were collected, with an average stratigraphic step of 0.5 m. In the Kilian and Paquier levels, higher resolution sampling (every 20 cm) was performed.

3.2. HAWK pyrolysis

The amount and type of organic matter and inorganic carbon present in the studied sections were analysed using the HAWK (Wildcat Technology) anhydrous pyrolysis carbon analysis system at the Lithospheric Organic Carbon (LOC) lab, Department of Geoscience, Aarhus University, Denmark. A total of 124 samples were analysed; one every meter along the section, with an increased resolution of one sample per 20 cm in the Kilian and Paquier level. Analysis was conducted on approximately 50 mg of sample. The samples were pyrolyzed at 300 °C for 3 min (generating S1 peak), followed by a ramp of 25 °C/ min up to 650 °C (generating the S2 peak). Subsequently, the oxidation phase begins with an isothermal stage at 300 °C (for 1 min) up to 850 °C with a temperature ramp of 25 °C/min, with 5 min hold time. Measurements were calibrated using the IFP 160000 standard. The accuracy and precision of measurements were better than 5%. Hawk pyrolysis provides parameters such as hydrogen index (HI, mg HC/ g TOC, HC = hydrocarbons), oxygen index (OI, mg CO_2/g TOC), Tmax (°C), total organic-carbon content (TOC, wt%), and total inorganic-carbon content (MINC, wt% equivalent of $CaCO_3$). TOC data have already been published in Wang et al. (2022).

3.3. Handheld XRF analyses

Al and Ti concentrations were measured by XRF analyses using a handheld XRF Bruker TITAN S1. A total of 124 rock-loose powdered samples of about 0.10 g were analysed. Each sample has been analysed three times with an acquisition time of 60 s. The XRF instrument has been calibrated using in-house loose powder reference material. Relative precision for Al and Ti is better than 10%.

3.4. Stable carbon isotope analyses

Carbonate carbon isotope ($\delta^{13}C_{carb}$) analyses were already presented in Wang et al. (2022). The analysis was done using a Sercon 20–22 gas source isotope ratio mass spectrometer at the University of Exeter Penryn Campus following routines outlined in detail by Ullmann et al. (2020). Bulk rock powder was weighed to 1 μg precision with a targeted nominal quantity of 500 μg carbonate and transferred into 4.5 mL borosilicate vials. After flushing with He for 80s, samples were reacted with 0.1 mL anhydrous phosphoric acid at 70 °C and resultant He-CO_2 mixtures analysed in continuous flow setup alongside two in-house standards (CAR, Carrara Marble and NCA, Namibian Carbonatite). Each batch comprises 80 samples and 30 standards, of which 22 are CAR (the first four measurements are used for instrument settling and calibration of signal yield, and only 18 measurements taken for isotope ratio determination) and 8 are NCA. Instrumental drift and bias were monitored using CAR and NCA and raw sample data corrected with a two-point calibration using the accepted values of the in-house standards, which were established by calibration with international certified reference materials (NBS-18, Co-8, and LSVEC). Reproducibility of the measurements as monitored by multiple analysis of CAR (2 s.d.; $n = 36$) is 0.07 ‰ for carbon isotope ratios and 0.18 ‰ for oxygen isotope ratios. Carbonate content of the bulk samples was determined using a transfer function of signal yield versus weight constructed from measurements of CAR, which is assumed to be 100% pure calcite. Resulting carbonate contents for NCA (2 s.d., $n = 15$) were 97.4 ± 1.0% over the course of measurements, with one anomalous result (deviation of 28 s.d. from mean) excluded.

Bulk organic matter carbon isotope ($\delta^{13}C_{org}$) analysis were measured on 124 decarbonated bulk rock powder using a Sercon Integra gas source stable isotope ratio mass spectrometer at the University of Exeter Penryn campus. Samples were weighed into tin capsules at 10 μg precision targeting a nominal amount of 200 μg of organic carbon. Batches of 70 samples were analysed together with 24 in-house standards, 16 of which are Alanine and 8 powdered bovine liver. Analogous to the carbonate measurements, these standards were previously calibrated against international standards (IAEA-N-1, IAEA-N-2, IAEA-LSVEC, IAEA-CH-6, and B2155) and used for two-point calibration of the isotope measurements and monitoring of instrumental drift. Reproducibility of the analyses (2 s.d.) is 0.1 ‰ or better for alanine ($n = 48$) and bovine liver ($n = 24$). Accuracy of the analyses was further checked by multiple analysis of in-house standards used at the British Geological Survey (SOIL A, B and C), giving $\delta^{13}C$ values and carbon contents indistinguishable from accepted values: SOIL A ($n = 10$, 2 s.d.): $\delta^{13}C = -26.24 \pm 0.14$, TOC = 9.7 ± 0.5%; SOIL B (n = 10, 2 s.d.): $\delta^{13}C = -24.27 \pm 0.16$, TOC = 2.95 ± 0.16%; SOIL C ($n = 8$, 2 s.d.): $\delta^{13}C = -17.72 \pm 0.52$, TOC = 0.79 ± 0.06%.

4. Results

4.1. Pyrolysis data

In all the analysed samples, well-developed Gaussian-shaped S2 peaks can be observed (S2 yield for most samples >0.5 mgHC/g rock), with only minor S1 peak (Supplementary Fig. S1). Production index or transformation ratio is <0.1, further indicating that the samples have not reached the generation stage. The Tmax values are relatively steady around an average value of 432 °C, with minimum value of 425 °C and maximum value of 435 °C, which is close to but below the oil window. Overall, all these factors clearly indicate that the organic matter is well-preserved and has not reached the oil window.

The average measured TOC value is 1.49%, with minimum and maximum values of 0.63% and 3.19%, respectively (Fig. 5). On a long-term perspective, TOC values increase from the base of the section to ca. 100 m in the section (HN 2 level), where they range around 1.75%. The remainder of the section is characterized by a subtle long-term decrease toward values ranging around 1.25% in the uppermost part of the section. Interrupting this long-term trend, there are three important peaks in TOC values associated with the Kilian, HN 8, and Paquier levels. Maximum TOC values around 2.2% are observed for both Kilian and HN 8 levels, whereas maximum TOC values reach 3.19% in the Paquier level. The other HN levels are also characterized by a slight enrichment in TOC value compared to background values. The total inorganic carbon content (MINC) values are comprised between 12.6 and 39.1% eq$CaCO_3$. An overall long-term decline in MINC values can be observed. Hence, MINC values are clustering around 30% in the lowermost part of the section, followed by a decline to 20% in its upper half.

Background HI values fluctuate between 30 and 75 mgHC/gTOC, whereas OI values have an average value of 50 mgCO_2/gTOC. Given that the kerogen is immature, this indicates that most of the preserved organic matter in this section is of continental origin (Figs. 5–6). A small long-term increase in HI values from the base to the top of the section is observed. Interrupting this background trend, several intervals of elevated HI values are observed. They correspond to the Kilian, HN 8, Paquier, HN 10, HN 11, HN 12, and HN 13 levels. In the Kilian, HN 8, HN 10, HN 11, and HN 12 levels, the HI values peak around 150 mgHC/gTOC, whereas in the HN 13 and Paquier levels, the HI values surpasses 250 mgHC/gTOC, with a maximum of 315 mgHC/gTOC reached in the

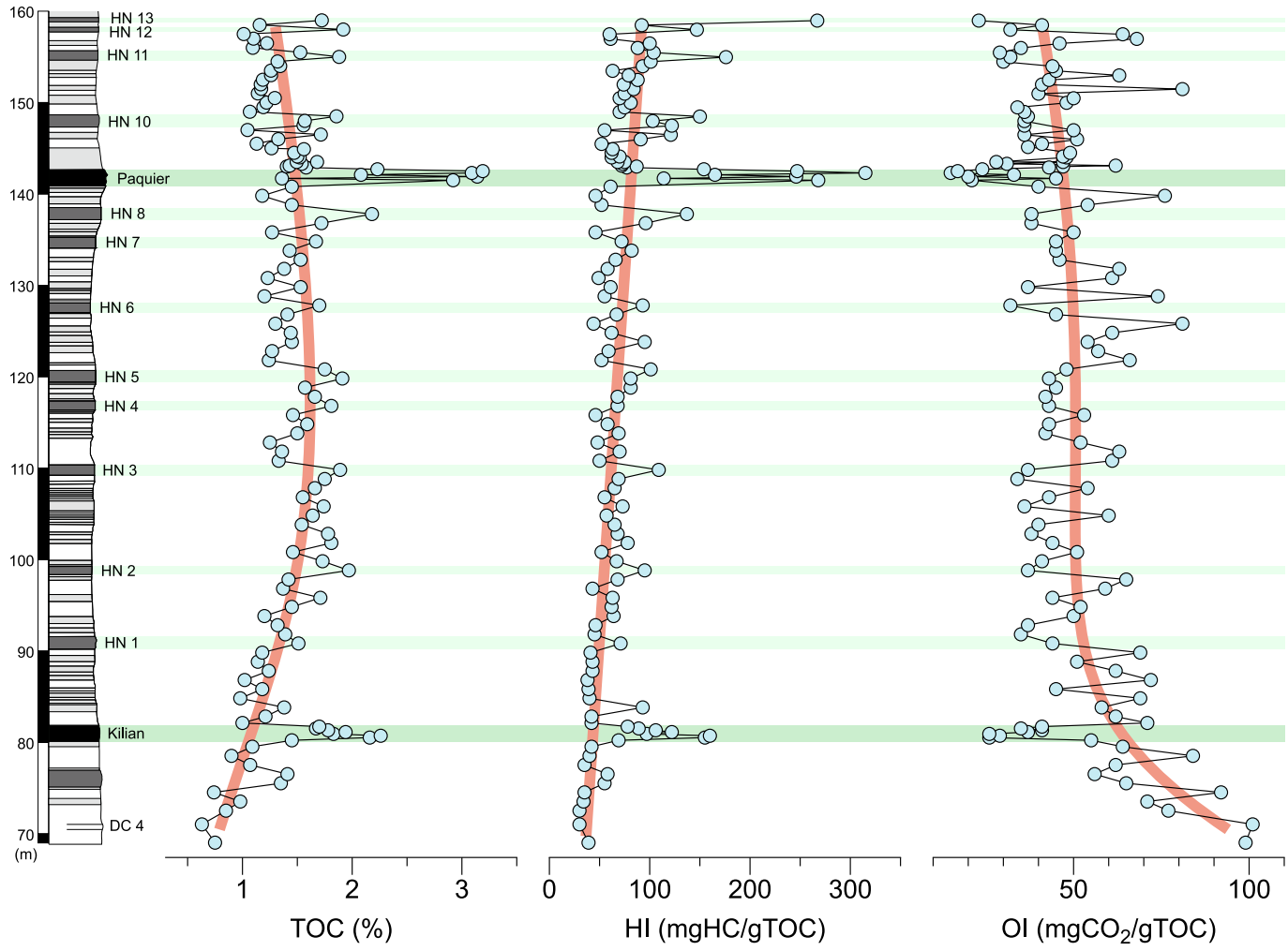

Fig. 5. Results from Hawk pyrolysis analyses (total organic carbon, hydrogen index, and oxygen index) plotted against stratigraphy. TOC data are from Wang et al. (2022). The red lines underline the long-term trend in TOC, HI, and OI data. (For interpretation of the references to colour in this figure legend, the reader is referred to the web version of this article.)

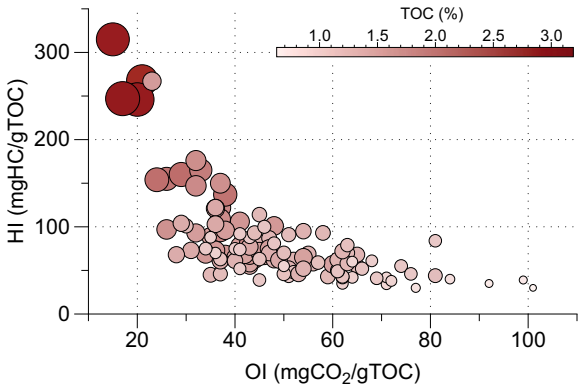

Fig. 6. Cross-plot of hydrogen index (HI) versus oxygen index (OI), with TOC content, illustrating the origin of the organic matter in the Briers section. Most of the data plot in the lower part of the diagram (HI < 150 mgHC/gTOC) indicating a type III (continental) organic matter. The spreading of the data cluster argues for mixing between continental and marine organic matter. The samples with higher HI values have also a higher TOC content, showing that preservation of marine organic matter is the principal reasons for high TOC values in the sub-levels of the OAE 1b cluster in the Vocontian Basin.

upper part of the Paquier level. These values indicate that marine organic matter is a substantial contributor of TOC preserved in these aforementioned levels. For the Paquier and the HN 13 levels, given their very high HI values, it is also most likely that marine organic matter is the main contributor to the TOC.

4.2. Stable isotope data

The average bulk rock $\delta^{13}C_{carb}$ and $\delta^{13}C_{org}$ values are 1.90‰ and −25.15‰, respectively. Both records follow a long-term decreasing trend, with an amplitude of 1.5‰ for the $\delta^{13}C_{carb}$ values and 2.5‰ for the $\delta^{13}C_{org}$ values (Fig. 7). Superimposed on this long-term decrease, a subdued positive bulge in both $\delta^{13}C_{carb}$ and $\delta^{13}C_{org}$ trend can moreover be inferred in the upper part of the section (from 120 m to the top), peaking around the Paquier level. Apart for the Paquier level, both curves show also similar medium-term changes, characterized by the occurrence of sinusoid $\delta^{13}C$ fluctuations spanning over 10–20 m (15 m on average) of stratigraphy. These rhythmic fluctuations have an average amplitude of 0.5‰ in the carbonate record, and 1‰ in the organic matter record. Minima in $\delta^{13}C$ values often coincide with HN levels.

The Kilian level is characterized by an asymmetric $\delta^{13}C$ excursion in both carbonate and organic matter, showing a sharp negative $\delta^{13}C$ shift at its onset, followed by a progressive return to pre-excursion values.

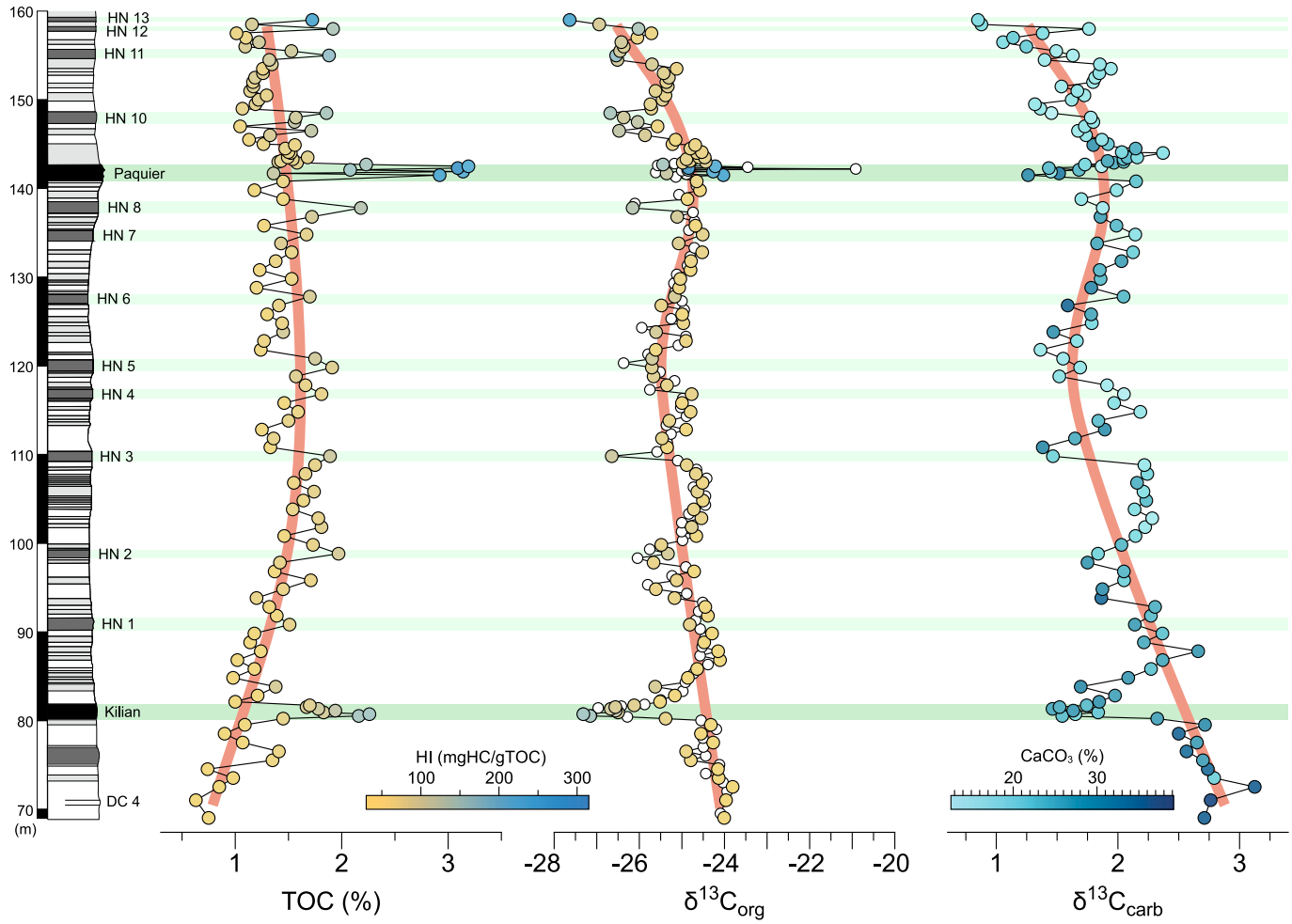

Fig. 7. Bulk organic matter and carbonate $\delta^{13}C$ values measured in the Briers section, compared to the stratigraphic evolution of TOC, HI, and carbonate (MINC) content values. $\delta^{13}C_{carb}$ data are from Wang et al. (2022). The red lines underline the long-term trend in the TOC, $\delta^{13}C_{carb}$, and $\delta^{13}C_{org}$ datasets. Note the similar long-term trend in between the $\delta^{13}C_{carb}$ and $\delta^{13}C_{org}$ records in this section, as well as with the $\delta^{13}C_{carb}$ reference curve (Fig. 3; Herrle et al., 2004). (For interpretation of the references to colour in this figure legend, the reader is referred to the web version of this article.)

The amplitude of the negative excursion is however different between the two records: it is of ca. 1‰ for the $\delta^{13}C_{carb}$ record whereas it reaches almost 3‰ in the $\delta^{13}C_{org}$ record. Similar to the Kilian level, the Paquier level is also characterized by a ca. 0.75‰ negative $\delta^{13}C_{carb}$ excursion, but the $\delta^{13}C_{org}$ record shows a pronounced positive excursion instead, with one value reaching −20.9‰. A similar dichotomy between the $\delta^{13}C_{carb}$ and $\delta^{13}C_{org}$ trends across the Paquier level has already been noted in the Vocontian Basin (Benamara et al., 2020), as well as in the Atlantic and Italian records (Kuypers et al., 2001; Trabucho Alexandre et al., 2011; Sabatino et al., 2015).

There is an overall good correlation between the $\delta^{13}C_{carb}$ results presented here and the reference curve established by Herrle et al. (2004) from a composite section in the north-western part of the Vocontian basin (Fig. 2). The prominent positive bulge of $\delta^{13}C_{carb}$ values observed by these authors around the Paquier is however not as well expressed in the Briers section though still observable. The ca. 1‰ negative $\delta^{13}C_{carb}$ shifts that are associated with the HN 3 and HN 5 levels in the Briers section can also be observed in the Herrle et al. (2004) record. Their presence can also be noted in our $\delta^{13}C_{org}$ record.

4.3. XRF data

Both Al and Ti content show similar trends (Fig. 8). A long-term increase in these two elements' content occurs from the base of the section to the stratigraphic interval between the HN 2 and HN 3 levels. This is followed by a stable to slightly decreasing long-term trend up to the top of the section, punctuated by medium-term rhythmic fluctuations. Hence, Al and Ti content curves show a first interval of high values centred between the HN 2 and HN 3 levels, a second around the HN 4 – HN 5 levels, and a last one around the Paquier – HN 10 levels interval. These medium-term Al and Ti fluctuations are anti-correlated with the carbonate content fluctuations measured from pyrolysis analyses (Figs. 8–9).

When excluding the Kilian, HN 8, and Paquier levels, which have elevated HI values compared to background trends, there is a good correlation between the Al and Ti content, and the TOC (Figs. 8–9). The long-term trend in Al and Ti content is hence similar to the long-term trend in TOC fluctuations. In the TOC vs. Al or Ti plot, it is also important to observe that the values of the three previously excluded intervals are for most of them reported above the correlation line, highlighting that for similar Al or Ti content as the background trend, these levels have substantially higher organic matter content.

5. Interpretations and discussion

5.1. Drivers of organic matter accumulation

Enrichment of sedimentary organic matter in marine sediments is the fundamental landmark of OAEs (Schlanger and Jenkyns, 1976). In most cases, the organic matter associated with Cretaceous OAEs is of marine

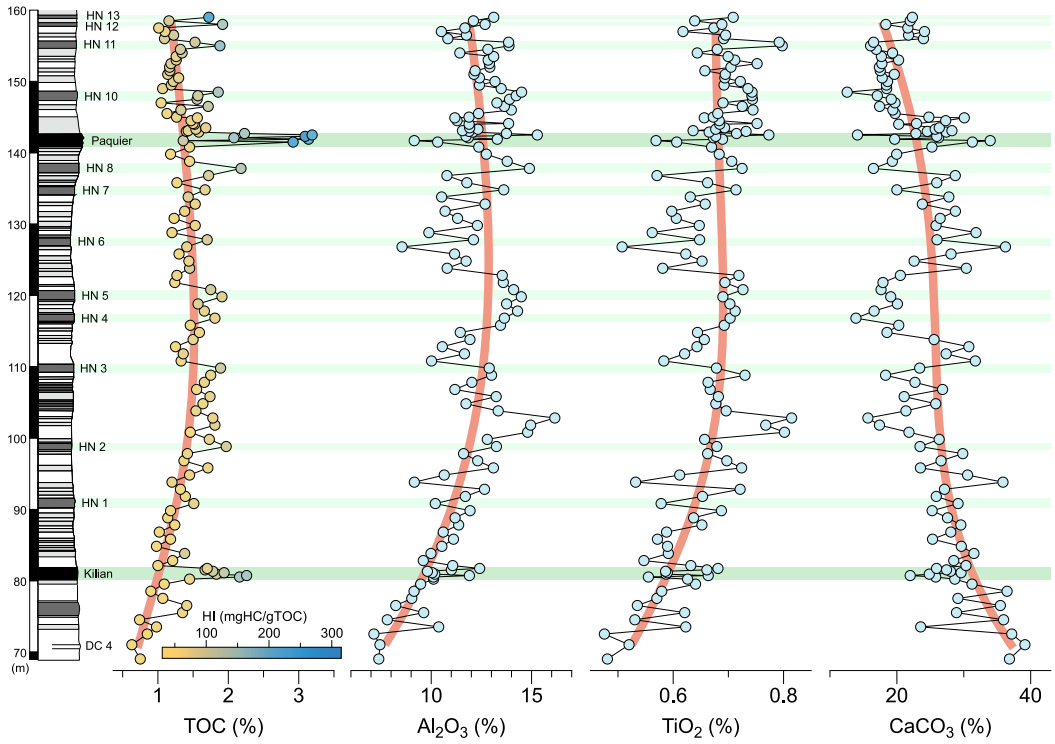

Fig. 8. XRF data (Al, Ti) measured in the Briers section, compared to the stratigraphic evolution of TOC, HI, and carbonate content values. The red lines underline the long-term trend in the TOC, Al, Ti, and $CaCO_3$ content datasets. (For interpretation of the references to colour in this figure legend, the reader is referred to the web version of this article.)

origin, leading to the postulation that these events were associated with increased marine primary productivity and/or preservation (e.g., Jenkyns, 1980, 2010; Mort et al., 2007a). The organic matter record for the OAE 1b cluster in the Briers section contrasts with this standard scenario as most of the organic matter is of continental origin, underlining once more the unconventional nature of this time interval, and/or its attribution to an OAE as defined in other stratigraphic intervals. Enrichment in marine organic matter is nonetheless also observed, but only for discrete stratigraphic intervals, out of which the Paquier level is the most pronounced one. In that sense, the Kilian, HN 8, and Paquier subevents are on their own better fitting the definition of an OAE, rather than their grouping within a cluster of events, i.e. OAE 1b.

In order to understand the environmental driver(s) of organic matter accumulation across the OAE 1b cluster (i.e., on a long-term scale), important information can be gained from the long-term correlation between the TOC and the Al or Ti contents, when excluding the data from the Kilian, HN 8, and Paquier levels (Fig. 9). Aluminium, and to a lesser extent Ti, are reliable indices of the detrital aluminosilicate component of sedimentary rocks, often used to normalize the concentration of other elements in sedimentary and soil analyses (e.g. Calvert, 1976; Riquier et al., 2006; Wei and Algeo, 2020). Hence, the Al and Ti trends through the section imply that the first 30 m of the section until the HN 2 level records a secular increase of siliciclastic content in the marls, followed by a long-term slow decrease until the top of the section. These changes in the siliciclastic/carbonate ratio could be related either to changes in the influx of siliciclastic material in the basin that can be linked to changes in continental runoff, and/or to changes in the strength of carbonate production and export to the sea-floor. Disentangling the two processes is not evident as it requires two independent proxies of sedimentary flux, i.e., one for each source of sediment type. We do not have an independent proxy for pelagic carbonate production in our dataset, limiting therefore the breath of this discussion. But, although fluctuation in the pelagic carbonate production might have occurred, we postulate that changes in continental runoff was the primordial reason behind the fluctuations in the Al and Ti content in the Briers section. Firstly, as deduced from the stratigraphic change in carbonate content (Fig. 8), the thickness of the carbonate-"poor" intervals is systematically higher than the thickness of the surrounding carbonate-"rich" intervals, which can be well understood in the case of a relatively constant pelagic carbonate flux diluted by fluctuating clastic input. Secondly, a change in continental runoff around the Vocontian Basin can also be inferred by the clay mineral dataset of the Col de Pré-Guittard (Corentin et al., 2020), where an increasing then decreasing trend in kaolinite content across the Kilian-Paquier stratigraphic interval is observed, similar to the long-term Al and Ti trends in our dataset. As kaolinite is formed under humid climate, this strongly supports the use of the Al and Ti content in the Briers section as a continental runoff tracer. As such, having in mind that the HI values indicate that the organic matter is mostly of continental origin, the correlation between Al or Ti contents with TOC contents (Fig. 9) indicates that the background accumulation of organic matter during the unfolding of OAE 1b is predominantly driven by the strength of continental erosion, and therefore the amount of continental organic matter brought into the Vocontian Basin by continental runoff. Long-term organic matter accumulation in the SE France Basin during the OAE 1b cluster was therefore likely linked to preservation and continental proximity rather than enhanced marine productivity processes. This might also explain the absence of substantial TOC enrichments throughout the OAE 1b cluster (beside the Jacob, Kilian, Monte Nerone, Paquier, and Leenhardt levels) in numerous Atlantic and Pacific localities (e.g., Robinson et al., 2004; McAnena et al., 2013), as these latter are situated far offshore and are hence relatively insensitive to continental clastic influx.

Compared to this background trend, the Kilian, HN 8, and Paquier levels are characterized by relatively elevated TOC values, as well as by a pronounced spike in HI values (Fig. 5). The supplementary amount of organic matter preserved in these levels is therefore directly linked to the addition of marine organic matter on top of the background continental organic matter accumulation. Given that marine organic matter is

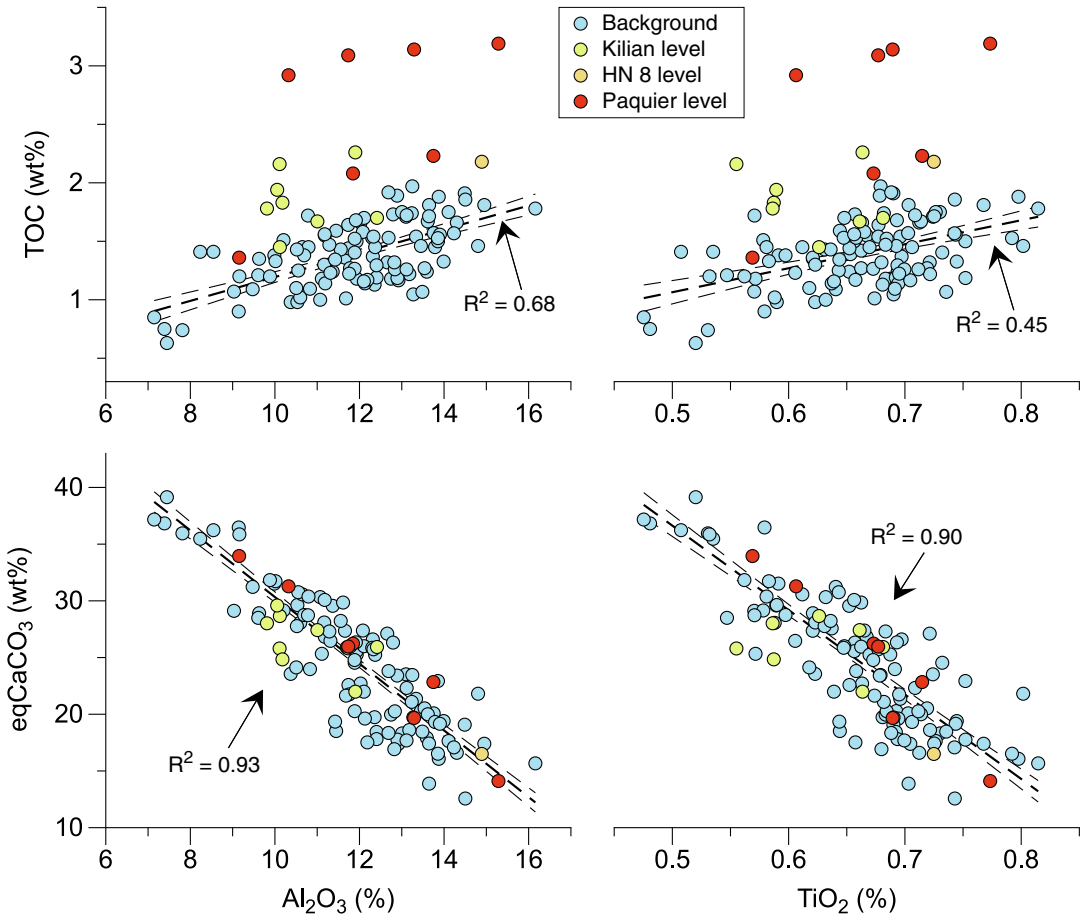

Fig. 9. Cross-plots of TOC and $CaCO_3$ content versus Al and Ti content. Data measured in the Kilian, HN 8, and Paquier levels have been separated from the other samples, assimilated here to background values. For the cross-plots with TOC values, the least square linear regression and coefficient of correlation (R^2) are calculated for the background samples only.

more labile than continental organic matter, these abnormal TOC values could result from two non-exclusive processes (e.g. Tyson, 2005; Mort et al., 2007b; MacQuaker et al., 2010). On the one hand, decreased organic matter remineralization due to decreased oxygen level could have been instrumental for these elevated organic matter contents (so-called preservation model; e.g., Bralower and Thierstein, 1984; Tessin et al., 2015). On the other hand, increased primary productivity outpacing the remineralization potential of the water column (so-called productivity model; e.g., Pedersen and Clavert, 1990; Kuypers et al., 2002) could as well explain the formation of these peculiar levels. Disentangling the role of these two mechanisms has always proven challenging (e.g., Mort et al., 2007b).

The preservation model invokes sluggish oceanic circulation as a cause for reduced deep-water ventilation (Bralower and Thierstein, 1984; Erbacher et al., 2001; Tessin et al., 2015). This favours deep-water anoxia, which is thus the primary cause for organic matter enrichment, without having to be necessarily related to enhanced primary productivity. The productivity model, on the other hand, invokes increased marine organic matter production as a result of enhanced nutrient levels as the primary cause for organic matter enrichment in the sediments (Jenkyns, 1980; Pedersen and Clavert, 1990; Kuypers et al., 2002). Hence, understanding nutrient level changes across the OAE 1b cluster in the Vocontian Basin is paramount for disentangling preservation from productivity as a primary cause for TOC enrichment. On geological time scales, phosphorus is the ultimate control on primary productivity (Tyrrell, 1999). Phosphorus is predominantly delivered to the ocean via continental weathering and runoff (Föllmi, 1996). As discussed before, in the Briers section, continental runoff can be tracked by the Al or Ti content. Small positive peaks of these elements can be observed within the Kilian, HN 8, or Paquier levels, although the absolute magnitude of these peaks is only minor compared to the long-term trend and other short-term fluctuations. This would suggest only minor increase of nutrient levels during the unfolding of these events. A somewhat different conclusion could be drawn from other datasets also established in the Vocontian Basin that, on the contrary, seem to indicate increased weathering and runoff during these events. The palynomorph TMR (terrestrial to marine ratio) index established in the l'Arboudeysse section indicates an increase of terrigenous input during the Paquier event (Herrle et al., 2003). Moreover, kaolinite abundance in the Col de Pré-Guittard section (Corentin et al., 2020) also increases associated with the Kilian, HN 8, and Paquier levels. It should, however, be noted that the above-mentioned positive peaks of kaolinite, like those observed in the Al and Ti content, have a magnitude lower than the one of the long-term positive excursions in which they are inscribed. An alternative mechanism for increasing oceanic nutrient levels on a regional scale is the development of upwelling currents. This mechanism cannot be invoked here as the Vocontian Basin was not situated on a western continental margin or in an equatorial position, and hence not in a setting prone to wind-driven upwelling. Also, the short duration of these levels (<100 kyr; e.g., Herrle and Mutterlose, 2003; Benamara et al., 2020) as well as their global occurrence, imply genetic mechanisms that can only be short-lived and widespread. Both requirements are hardly met by the upwelling scenario. Altogether, we can infer that sporadic increase of nutrient levels due to pulses in continental runoff occurred during the unfolding of these events, but it is difficult to conclude that this was the sole driving factor behind the enhanced accumulation of

organic matter.

Hence, the addition of enhanced organic matter preservation is needed to explains the formation of the organic-rich levels in the Vocontian Basin, as well as on a global scale (Erbacher et al., 2001; Herrle and Mutterlose, 2003). This enhanced preservation of organic matter was favoured by dysoxia/anoxia of the seafloor as deduced from enrichment of redox sensitive trace metals in the Kilian and Paquier levels (Benamara et al., 2020; Wang et al., 2022). Increased thermohaline stratification, limiting the ventilation of bottom water masses, was previously invoked as a cause for the accumulation of organic matter within the Paquier level in the Atlantic Ocean (Erbacher et al., 2001). A similar scenario can also be inferred in the Vocontian Basin given that the Kilian, HN 8, and Paquier levels are associated with higher seawater temperature (Herrle and Mutterlose, 2003; Herrle et al., 2003). Once bottom-water anoxia is established, the recycling of sediment-bound phosphorus would also provide a positive feedback loop, triggering further organic matter production and preservation (Benamara et al., 2020), as commonly observed in other Mesozoic OAEs (e.g., Bodin et al., 2006; Mort et al., 2007a; Stein et al., 2011; Fantasia et al., 2018). Moreover, this increased nutrient level could also explain the rise of archaea primary productivity during the Paquier level (Kuypers et al., 2001).

To summarize, the short-lived increased TOC values in the Vocontian Basin associated with the Kilian, HN 8, and Paquier levels, are most likely the result of combined short-lived events of increased marine primary production and organic matter preservation, superimposed over a long-term period of enhanced continental organic matter delivery to the Vocontian Basin during the latest Aptian–early Albian. This long-term period of increased riverine flux around the Vocontian Basin is correlated to a global increase of continental weathering as indicated by the positive trend in marine $^{87}Sr/^{86}Sr$ and $^{187}Os/^{188}Os$ ratios during this time interval (Wang et al., 2022; Matsumoto et al., 2023). A combination of both local and global processes therefore best explains the occurrence of organic matter-rich interval in the Vocontian Basin and elsewhere.

5.2. *Influence of organic matter type on the $\delta^{13}C_{org}$ record*

Due to differential carbon isotope fractionation among distinctive types of organic matter, bulk organic matter $\delta^{13}C$ records can be strongly influenced by organic matter sourcing (Sluijs and Dickens, 2012; Suan et al., 2015). During the Mesozoic, a well-documented example of this mixing effect is recognized during the Toarcian OAE, where the admixture of marine organic matter in the bulk record substantially amplifies the negative $\delta^{13}C$ excursion characteristic of this event (Suan et al., 2015). In the Briers record, the amplitude of the negative $\delta^{13}C_{org}$ excursions recorded in the Kilian, HN 2, HN 3, HN 4–5, HN 8, HN 10, HN 11, and HN 13 levels are approximately double than the one observed in the $\delta^{13}C_{carb}$ record. Moreover, the $\delta^{13}C_{org}$ record across the Paquier level shows a positive excursion whereas its $\delta^{13}C_{carb}$ record shows a negative excursion. These observations either point at intricate changes in the carbon cycle between the carbonate and organic matter carbon isotope fractionation during these events, or to processes related to carbonate or organic matter sourcing. The following rationale argues in favour of the organic matter sourcing hypothesis.

We believe that changes in carbonate sourcing are not influencing the $\delta13C_{carb}$ record in the Briers section because during the Aptian–Albian transition there were no productive neritic carbonate areas around the Vocontian Basin, therefore ruling out any carbonate export from shallow-marine environments. Pelagic carbonate productivity is consequently likely to account for most of the carbonate present in the Blue Marls Formation. This assumption is reinforced by the fact that the Aptian–Albian transition marks also the onset of the chalk sea in the Tethys and North Atlantic (Giorgioni et al., 2015), and hence of vigorous pelagic carbonate production. We also note that there is an absence of correlation between the bulk carbonate carbon isotope record and the carbonate content in our section, as well as the similarity of $\delta^{13}C_{carb}$ records across different basins (e.g., Coccioni et al., 2014). Together, these observations strongly support the notion that the $\delta^{13}C_{carb}$ record of the Vocontian Basin is not substantially influenced by source changes and therefore a reliable tracer for marine carbon cycle change. The same cannot be said for the organic matter carbon isotope record. As a matter of fact, we note that a gross linear relationship between $\delta^{13}C_{org}$ and HI values can be observed in our record (Fig. 10). This hints at an influence of organic matter type on the carbon isotope record. We therefore propose to use the same methodology as the one presented in Suan et al. (2015) in order to extract a corrected $\delta^{13}C_{org}$ dataset ($\delta^{13}C^*_{org}$) that represent the hypothetical change which would be observed in bulk organic matter $\delta^{13}C$ values if this latter would only be composed of one type of organic matter, i.e., not influenced by organic matter mixing. To correct the $\delta^{13}C_{org}$ fluctuations from this parameter, we used the slope and intercept of the HI-$\delta^{13}C_{org}$ regression line (Table 1), excluding the Paquier and the HN 13 levels data as their organic matter are of a peculiar, third type (see below). The $\delta^{13}C^*_{org}$ values can thus be calculated for the rest of the dataset, according to the following equations:

$$\delta^{13}C^*_{org} = \delta^{13}C_{org} - \delta^{13}C_{HI} + c$$

$$\delta^{13}C_{HI} = HI * a + b$$

where $\delta^{13}C_{HI}$ is the $\delta^{13}C$ expected if changes in HI values was the only parameter controlling the bulk organic matter carbon isotope ratio, a and b are the slope and intercept of the HI-$\delta^{13}C_{org}$ least square regression lines (Fig. 10), and c is the $\delta^{13}C_{org}$ value of the sample with the lowest HI value in this survey (i.e. $c = -23.96‰$, HI = 30 mgHC/gTOC). Doing this exercise for several HI-$\delta^{13}C_{org}$ regression lines, all calculated by excluding different "perturbed" intervals (Table 1) gives us an envelope of $\delta^{13}C^*_{org}$ values that can be used as an appreciation for the uncertainty of this method. This latter is very small, with a mean value of 0.08‰ ($\sigma = 0.06‰$). Noting that the Kilian–Paquier levels interval is also characterized by a long-term trend of declining $\delta^{13}C$ values which could partly contribute to the gross linear relationship between $\delta^{13}C_{org}$ and HI values, the same calculation was applied to a detrended $\delta^{13}C_{org}$ dataset (Table 1). It should be noted however that this correction method underestimates the role of changing HI values in driving $\delta^{13}C_{org}$ fluctuations because it neglects the long-term increase in HI value through the Briers section (Fig. 5). Detrending the $\delta^{13}C_{org}$ dataset for calculating $\delta^{13}C^*_{org}$ values represent thus an extreme case scenario. Including this corrected dataset (Table 1) gives an envelope of $\delta^{13}C^*_{org}$ curves that has average spread of 0.16‰ ($\sigma = 0.12‰$; Fig. 11), which is still negligible compared to the overall fluctuations of the corrected dataset.

In the obtained $\delta^{13}C^*_{org}$ curves, the amplitude and shape associated with the different negative and positive excursions are substantially reduced compared to the original $\delta^{13}C_{org}$ curve, even in the case using detrended $\delta^{13}C_{org}$ values (Fig. 11). Interestingly, these corrected amplitudes are now more similar to the ones observed in the $\delta^{13}C_{carb}$ curve, confirming that the original $\delta^{13}C_{org}$ values are indeed substantially influenced by organic matter sourcing. Moreover, given that the $\delta^{13}C^*_{org}$ is corrected for the influence of marine organic matter, it hence represents fluctuations of the continental organic matter $\delta^{13}C$ record. As such, it also represents variation in the carbon isotopic content of the atmosphere. Given the short (ca. 1 year) mixing time of the atmosphere, this isotopic signal is therefore uniform across the globe and at equilibrium with the upper ocean on sub-Milankovitch timescale. Thus, the similarity between the short-term fluctuations in the $\delta^{13}C_{carb}$ and $\delta^{13}C^*_{org}$ curves highlights that the carbon cycle perturbations at the origin of these $\delta^{13}C$ changes were global, affecting the entire ocean/atmosphere/biosphere carbon reservoirs. This reinforces the notion that high-precision $\delta^{13}C$ curves across the Aptian/Albian boundary interval can be used as a powerful chemostratigraphic tool in both marine and terrestrial records, as already demonstrated by the precise high-resolution chemostratigraphic correlation between France, Italy, and the Canadian High Arctic (e.g., Herrle et al., 2015; Sabatino et al., 2015).

A positive excursion in the $\delta^{13}C_{org}$ record for the Paquier level was

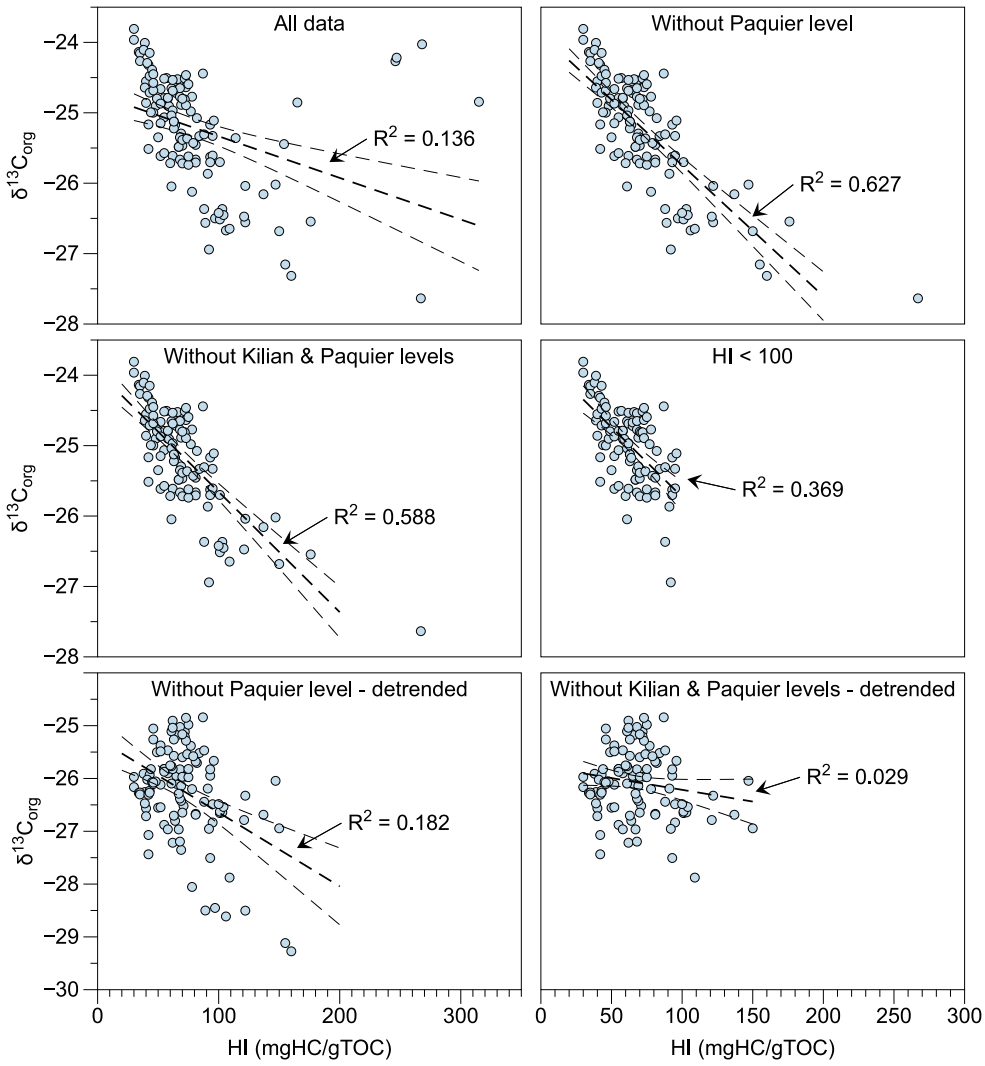

Fig. 10. Cross-plots between $\delta^{13}C_{org}$ and HI values. Different subsets of data are presented (see text for discussion). Least square linear regression data are detailed in Table 1.

initially reported by Kuypers et al. (2001) in the ODP site 1049C. This ca. 5‰ positive $\delta^{13}C_{org}$ excursion is in strong contrast with the small negative excursion reported for the same level in the carbonate tests of planktic foraminifera (Erbacher et al., 1999, 2001). This strong decoupling between both records, together with the presence of specific archaeal molecular fossils with high $\delta^{13}C$ values (ca. −17‰) in the Paquier level and the occurrence of a negative $\delta^{13}C$ excursion in isolated algal steranes, indicates that in the ODP site 1049C, the Paquier level $\delta^{13}C_{org}$ positive excursion is linked to a change in the relative contribution between algal and archaeal organic matter during the Paquier event (Kuypers et al., 2001). Similar positive $\delta^{13}C_{org}$ excursions in the Paquier level were later recognized in other Atlantic localities (Trabucho Alexandre et al., 2011), as well as in Italy (Sabatino et al., 2015) and the Vocontian Basin (Benamara et al., 2020). It seems therefore that this unusual $\delta^{13}C_{org}$ excursion is a supra-regional feature, which could indicate that substantial development of marine archaea over the Atlantic and Tethys Oceans occurred during the Paquier event. Under this scenario, assuming that our $\delta^{13}C_{carb}$ record in the Briers section accurately tracks changes in the exogenic carbon isotopes cycle, and a value of −17‰ for the marine archaea carbon isotope ratio (Kuypers et al., 2001), a two end-members mass balance calculation indicates that on average, around 25% (maximal value of 56%) of the Paquier level organic matter of this level is of archaeal origin. This average value is lower than those calculated for the Atlantic and Italian records (Kuypers et al., 2001; Sabatino et al., 2015), but compares well with the value that was calculated for the L'Arboudeysse section in the NW part of the Vocontian Basin (Benamara et al., 2020). Alternatively, these anomalous $\delta^{13}C_{org}$ values in the Paquier level could also be related to the presence of sulfurized organic matter, as this latter is typically 4–10 ‰ heavier than algal lipids (Sinninghe Damsté et al., 1998). Biomarker study would be required here to decipher between these two options, but this is beyond the scope of our study. In all cases, the anomalously positive $\delta^{13}C_{org}$ values in the Paquier level indicate the presence of an uncommon type of ^{13}C-enriched organic matter.

A comparable positive excursion in $\delta^{13}C_{org}$ values is also observed in the Kilian level in Italy (Sabatino et al., 2015), but has not been observed elsewhere so far. It is therefore likely that the unfolding of the Kilian event was thus also accompanied by the expansion of marine archaea or enhanced preservation of sulfurized organic matter, but only on a restricted, regional scale. Moreover, the $\delta^{13}C_{org}$ value of the HN 13 level in the Briers section, although being the lowest value of our dataset, is nonetheless relatively elevated compared to its high HI value. When $\delta^{13}C^{*}_{org}$ values are calculated for this interval, they average around −22.8‰ and are hence not in tune with the observed $\delta^{13}C_{carb}$ changes. Consequently, similar to the Paquier level, the HN 13 level is most likely also characterized by the substantial presence of archaeal or sulfurized organic matter. Overall, these observations suggest that the sporadic bloom of marine archaea might have taken place at several occasions

Table 1
Slope (a), intercept (b), least square regression coefficient (R^2), and number of sampled considered (n) for different scenario of "perturbed" intervals exclusion. Colour refer to the $\delta^{13}C^*_{org}$ curves displayed in Fig. 12.

Original data	Interval excluded	a	b	R2	n	Colour in Fig. 11
All data	n/a	−0.0059	−24.742	0.1362	124	n/a
Without Paquier level	141.5 m–142.7 m	−0.0186	−23.885	0.6269	117	Green
Without Paquier and Kilian levels	80.2 m–81.7 m & 141.5 m–142.7 m	−0.0171	−23.947	0.5881	109	Red
Only when HI <100		−0.0198	−23.752	0.3689	96	Blue
Detrended data						
All data	n/a	−0.0008	−26.13	0.0018	124	n/a
Without Paquier level and outliers	141.5 m–142.7 m	−0.014	−25.246	0.1817	115	orange
Without Paquier and kilian levels, and outliers	80.2 m–81.7 m & 141.5 m–142.7 m	−0.0045	−25.77	0.036	108	n/a

during the Aptian/Albian boundary interval, highlighting the need of further research for understanding the exact environmental conditions leading to the development of these peculiar marine, non-thermophilic archaea.

5.3. A dynamic carbon cycle across the Kilian–Paquier events interval

On a short-term scale, the similarity between the $\delta^{13}C^*_{org}$ and $\delta^{13}C_{carb}$ records highlights that the mechanism at the origin of these isotopic fluctuations was affecting both oceanic and atmospheric reservoirs and was hence of global nature (cf. previous chapter). One striking aspect of these carbon isotope fluctuations is their rhythmicity, which can be linked to the expression of precessional cycles by comparison to other cyclostratigraphic studies undertaken in the Blue Marls Formation (Herrle and Mutterlose, 2003; Gale et al., 2011; Ghirardi et al., 2014). Cyclic fluctuations of carbon isotopic records have long been noticed in the Mesozoic – Cenozoic (e.g. Cramer et al., 2003; Pälike et al., 2006; Holbourn et al., 2007; Voigt et al., 2007; Giorgioni et al., 2012; Storm et al., 2020), and are thought to reflect astronomically-paced modifications in the partitioning of carbon between oxidized and reduced reservoirs. But which exact mechanisms can here be invoked?

A first observation of peculiar interest in this regard is the dichotomy between the occurrence of organic matter accumulation levels in the Vocontian Basin and global carbon cycle perturbations as documented by $\delta^{13}C$ records. As a matter of fact, numerous HN levels are not characterized by any peculiar perturbation of the $\delta^{13}C$ records. This is the case for HN 1, HN 4, HN 6, and HN 7. Moreover, some $\delta^{13}C$ perturbations are initiated and/or culminate out of tune with the HN levels, such as the large negative shift starting at 93 m in the section, above the HN 1 level, and well below the HN 2 level. This is also the case for the negative shift encompassing the HN 4 and 5 levels. The origin of these aforementioned levels is hence not related to global changes in carbon cycle, but to regional processes, which also explains their absence in other basins. On the other hand, as already demonstrated by Herrle et al. (2004), there is a good temporal correlation between the onset of the Kilian and Paquier levels with carbon cycle perturbations, as well as for the HN 3 level, which corresponds to the onset of the Monte Nerone level in Italy (Coccioni et al., 2014). A relatively sharp and pronounced >1‰ negative $\delta^{13}C$ shift in both $\delta^{13}C_{carb}$ and $\delta^{13}C^*_{org}$ records is associated with these three levels, followed by a longer-term return to pre-excursion values. This isotopic trend is somewhat counter-intuitive given the supra-regional to global occurrence of these levels, especially for the Kilian and Paquier levels. Indeed, as these latter are recording an increase of global burial of marine organic matter, one would expect them to be associated with a positive $\delta^{13}C$ excursion rather than a negative one. This contradiction can however be resolved in the light of the monsoonal mechanism postulated to explain the development of these levels in the first place (e.g., Herrle et al., 2003).

Linking astronomically-paced variations in the global carbon cycle with fluctuations of the monsoonal system has been on numerous occasions proposed and modelled for the Cenozoic record (Cramer et al., 2003; Pälike et al., 2006; Holbourn et al., 2007; Ma et al., 2011). As developed by Zachos et al. (2010) for the Paleogene, such a link can be understood by the involvement of continental organic matter deposited in wetlands, which would respond to the fluctuation of monsoonal precipitation and provide feedback on the carbon cycle. We hypothesize that similar mechanisms were also at work during the unfolding of the OAE 1b cluster (Fig. 12). This is based on the given estimated duration of ca. 2 Myr for the duration of the interval between the Kilian and Paquier levels (Gale et al., 2020), as well as the cyclic character of the TOC in the Briers section (Wang et al., 2022), which let us to propose that the long-term eccentricity cycle (405 kyr in duration) could be at the origin of these precipitation pattern fluctuations. In details, during eccentricity minima, weaker seasonal contrasts in low latitudes are dampening monsoonal activity (Crowley et al., 1992), leading to a more uniform repartition of yearly precipitation. This state is favourable to the accumulation of continental organic matter in wetlands, inducing as such an increase of organic carbon burial and hence, a positive $\delta^{13}C$ excursion in the exogenic carbon reservoir. On the other hand, during the transition to eccentricity maxima, intense but brief wet seasons, followed by prolonged dry seasons, are favoured. This promotes the desiccation of the wetlands and induces oxidation of the organic matter via wildfires, which is released as CO_2 in the atmosphere. This prevents ^{13}C-depleted carbon to be extracted from the exogenic carbon reservoir and is as such responsible for the global negative shifts in the $\delta^{13}C_{carb}$ and $\delta^{13}C^*_{org}$ records. Furthermore, this strong seasonality would have also favoured continental weathering (Ma et al., 2011), and as such the fertilization of the ocean and the seasonal bloom of marine bioproductivity, ultimately responsible for the deposition of organic matter layers in marine environment prone to anoxia (Fig. 12). This scenario is compatible with the observation that the Kilian, Monte Nerone, and Paquier levels are associated with increased global temperature in the Tethyan area (Wagner et al., 2008; Herrle et al., 2003; McAnena et al., 2013; Bottini and Erba, 2018) and negative carbon isotope excursions. It is also in full agreement with the observation from the Asian continent sedimentary record that increased wildfire activity has occurred during the Kilian, Paquier, and Leenhardt levels (Xu et al., 2022). Overall, this scenario implies that wetlands (and terrestrial areas in general) were assuming a substantial role in the driving of Middle Cretaceous climates, as also recently suggested by Hay et al. (2019). The vast continental areas of North America and Asia, which were the loci of these monsoonal climates (Herrle et al., 2003), have accommodated large river and lakes systems during the Mesozoic (e.g., Ludvigson et al., 2015; Suarez et al., 2018; Xu et al., 2022), providing as such the necessary conditions for this monsoon-wetland mechanism.

When replaced into a long-term perspective, the most striking feature about the stratigraphic position of the OAE 1b cluster is its occurrence at the end of the late Aptian cold interlude (Bodin et al., 2015; O'Brien et al., 2017; Bottini and Erba, 2018; Alley et al., 2020). This cold climate time interval was likely initiated by a long-term global

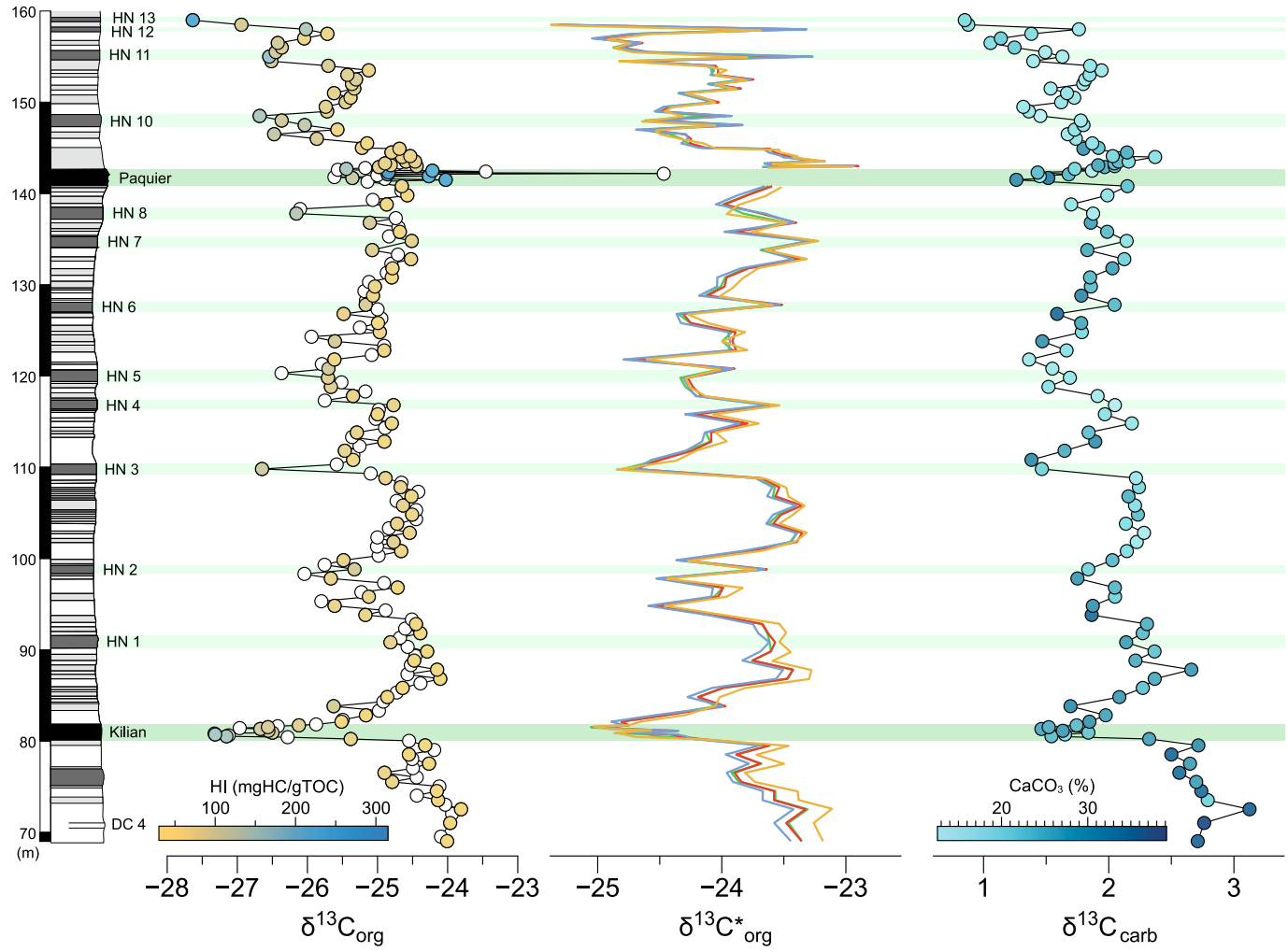

Fig. 11. Comparison between the measured $\delta^{13}C_{org}$ and $\delta^{13}C_{carb}$ records and the $\delta^{13}C^{*}_{org}$ values (green, red, blue, and orange curves; calculated using four different samples subsets that show a negative correlation between $\delta^{13}C_{org}$ and HI values, cf. Table 1 and Fig. 10). (For interpretation of the references to colour in this figure legend, the reader is referred to the web version of this article.)

increase of organic matter burial, as testified by a protracted positive $\delta^{13}C$ excursion during the late Aptian (Herrle et al., 2004, 2015; McAnena et al., 2013; Bodin et al., 2015), responsible for a lowering of atmospheric pCO_2 (Harper et al., 2021). The following OAE 1b cluster is inscribed within the stratigraphic interval covering the return to pre-excursion $\delta^{13}C$ values, signifying that on a long-term perspective, its unfolding was concomitant to an overall reduction of global organic matter burial, which would have promoted the building up of atmospheric pCO_2. The cause of this reduction in global organic matter burial is not well understood at the moment since an increase in continental weathering, and hence nutrient delivery in the ocean occurred in the early Albian (Wang et al., 2022; Matsumoto et al., 2023). It is here interesting to note that repeated Hg anomalies within the OAE 1b cluster in Italy and France suggest a link with a multi-phased emplacement of the Southern Kerguelen Plateau (Sabatino et al., 2018; Bracquart et al., 2022). This link was recently confirmed by Matsumoto et al. (2020) based on the presence of two negative Os isotopic spikes prior to the unfolding of the Kilian event, at the onset of the long-term decline in the $\delta^{13}C$ record. In general, the return to a greenhouse climate mode across the Aptian/Albian boundary interval could have diminished the ventilation of bottom water masses, which were thus prone to intermittent dysoxic/anoxic conditions. Such conditions could hence be reached in tune with orbitally-paced temperature changes and their effect on the monsoonal system and oceanic thermohaline stratification (Erbacher et al., 2001; Herrle et al., 2003; Wang et al., 2022), leading to the deposition of the OAE 1b sub-levels. Modelling also suggests that injection of greenhouse gases (CO_2 or CH_4) could have triggered the Kilian event (Wagner et al., 2007), potentially in link to feedback mechanism following the emplacement of the Southern Kerguelen Plateau (Matsumoto et al., 2020), but this remains to be verified for the other sub-events.

6. Conclusion

The OAE 1b cluster in the Vocontian Basin stands out from other Cretaceous OAEs as most of the preserved organic matter is of continental origin. The correlation between Al or Ti and TOC contents along with HI values, which indicate a continental origin of the organic matter, shows that fluctuation in continental erosion is the main driver of the background accumulation of organic matter during the unfolding of the OAE 1b. This long-term accumulation of continental organic matter into the Vocontian Basin is therefore linked to preservation and continental proximity rather than enhanced marine productivity processes. Nonetheless, marine organic matter enrichments observed in the Kilian, HN8 and Paquier sub-events can be explained by enhanced primary productivity linked to increased continental weathering and preservation of marine organic matter due to an increased thermohaline stratification. Hence, there is a superimposition of short events of increased marine organic matter preservation within a long-term period of continental organic matter delivery to the Vocontian Basin during the unfolding of

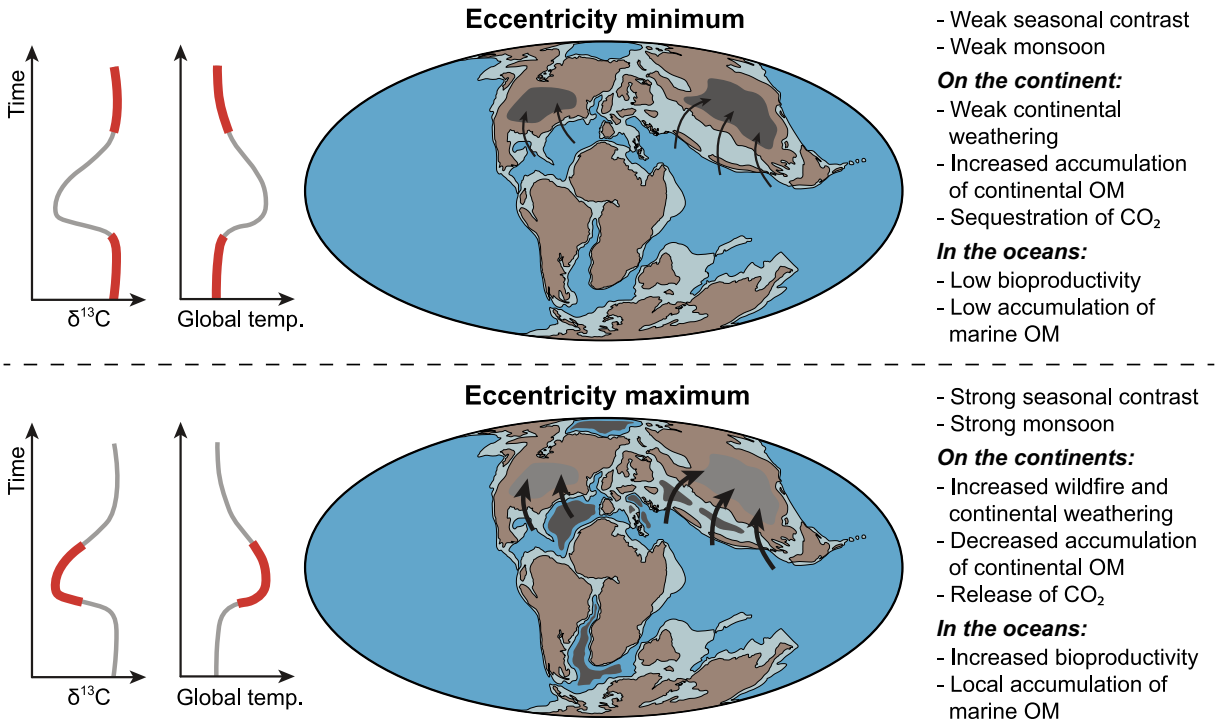

Fig. 12. Conceptual model linking eccentricity-paced fluctuations in monsoon strength and global perturbation of the carbon cycle (see text for details). Early Albian paleogeographic map modified after Scotese (2016). The black arrows represent monsoonal winds. This model implies a rhythmic, Milankovitch-paced change in the locus of organic matter burial between the continental and marine realms.

the OAE 1b cluster.

As shown by the similarities between $\delta^{13}C^{*}_{org}$ and $\delta^{13}C_{carb}$ curves, carbon isotopic fluctuations observed within the OAE 1b cluster are the results of global carbon cycle perturbations affecting the entire ocean/atmosphere system. As suggested by the rhythmic fluctuations of both $\delta^{13}C^{*}_{org}$ and $\delta^{13}C_{carb}$, these global changes seem to be the result of astronomical-driven variations affecting the monsoonal system, leading to a modification of wetlands organic matter distribution throughout the Aptian/Albian boundary interval. On the other hand, the origin of various sub-events only found in the Vocontian Basin is better explained by regional processes than global perturbations in carbon cycle. During the Paquier sub-event, supra-regional $\delta^{13}C_{org}$ positive excursion is explained by a contribution of archaeal organic matter or enhanced burial of sulfurized organic matter, which is also observed on a more restricted scale for the Kilian and HN13 sub-events. Further studies could highlight the processes that led to these sporadic production of unusual organic matter during the Aptian/Albian boundary interval.

Declaration of Competing Interest

The authors declare that they have no known competing financial interests or personal relationships that could have appeared to influence the work reported in this paper.

Data availability

Data will be made available on request.

Acknowledgments

We warmly thank Myette Guiomar and Didier Bert from the Reserve Géologique de Haute-Provence for providing fieldwork and sampling permits. We thank Paula Engell Sørensen and Alicia Fantasia for their help in the field. This manuscript has benefited from the constructive comments of two anonymous reviewers. This research was financed by the Aarhus Universitets Forskningsfond (grant n° AUFF-E-2015-FLS-8-77) to Stéphane Bodin.

Appendix A. Supplementary data

Supplementary data to this article can be found online at https://doi.org/10.1016/j.gloplacha.2023.104074.

References

Alley, N.F., Hore, S.B., Frakes, L.A., 2020. Glaciations at high-latitude Southern Australia during the Early Cretaceous. Aust. J. Earth Sci. 67, 1045–1095.
Ando, A., Kakegawa, T., 2007. Carbon isotope records of terrestrial organic matter and occurrence of planktonic foraminifera from the Albian stage of Hokkaido, Japan: ocean-atmosphere d13C trends and chronostratigraphic implications. Palaios 22 (4), 417–432.
Arnaud, H., 2005. The South-East France Basin (SFB) and its Mesozoic evolution. In: Adatte, T., Arnaud-Vanneau, A., Arnaud, H., Blanc-Aletru, M.C., Bodin, S., Carrio-Schaffhauser, E., Föllmi, K.B., Godet, A., Raddadi, M.C., Vermeulen, J. (Eds.), The Hauterivian – Lower Aptian Sequence Stratigraphy from Jura Platform to Vocontian Basin: A Multidisciplinary Approach, pp. 5–28.
Arthur, M.A., Jenkyns, H.C., Brumsack, H.-J., Schlanger, S.O., 1990. Stratigraphy, geochemistry and paleoceanography of organic-rich Cretaceous sequences. In: Ginsburg, R.N., Beaudoin, B. (Eds.), Cretaceous Resources, Events and Rhythms, NATO ASI Series, Serie C: Mathematical and Physical Sciences, 304. Kluwer Academic Publishers, Netherlands, pp. 75–119.
Ben Chaabane, N., Khemiri, F., Soussi, M., Latil, J.-L., Robert, E., Belhajtaher, I., 2019. Aptian-Lower Albian Serdj carbonate platform of the Tunisian Atlas: development, demise and petroleum implication. Mar. Pet. Geol. 101, 566–591.
Benamara, A., Charbonnier, G., Adatte, T., Spangenberg, J.E., Föllmi, K.B., 2020. Precession-driven monsoonal activity controlled the development of the early Albian Paquier oceanic anoxic event (OAE1b): evidence from the Vocontian Basin, SE France. Palaeogeogr. Palaeoclimatol. Palaeoecol. 537, 109406.
Bodin, S., Godet, A., Föllmi, K.B., Vermeulen, J., Arnaud, H., Strasser, A., Fiet, N., Adatte, T., 2006. The Late Hauterivian Faraoni oceanic anoxic event in the western Tethys: evidence from phosphorus burial rates. Palaeogeogr. Palaeoclimatol. Palaeoecol. 235, 245–264.
Bodin, S., Meissner, P., Janssen, N.M.M., Steuber, T., Mutterlose, J., 2015. Large igneous provinces and organic carbon burial: controls on global temperature and continental weathering during the Early Cretaceous. Glob. Planet. Chang. 133, 238–253.
Bottini, C., Erba, E., 2018. Mid-Cretaceous paleoenvironmental changes in the western Tethys. Clim. Past 14, 1147–1163.

Bracquart, E., Charbonnier, G., Garel, S., Munier, T., Adatte, T., Danzelle, J., 2022. New evidences of subaerial volcanism as a trigger for the Kilian event (Aptian-Albian transition) and major climatic changes from offshore Morocco (DSDP Site 545). Glob. Planet. Chang. 218, 103959.
Bralower, T.J., Thierstein, H.R., 1984. Low productivity and slow deep-water circulation in mid-Cretaceous oceans. Geology 12, 614–618.
Bralower, T.J., Sliter, W.V., Arthur, M.A., Leckie, R.M., Allard, D., Schlanger, S.O., 1993. Dysoxic/anoxic episodes in the Aptian-Albian (Early Cretaceous). In: Pringle, M.S., Sager, W.W., Sliter, W.V., Stein, S. (Eds.), The Mesozoic Pacific: Geology, Tectonics, and Volcanism, Geophysical Monograph Series, pp. 5–37.
Bralower, T.J., CoBabe, E., Clement, B., Sliter, W.V., Osburn, C.L., Longoria, J., 1999. The record of global change in mid-Cretaceous (Barremian-Albian) sections from the Sierra Madre, northeastern Mexico. J. Foraminifer. Res. 29, 418–437.
Bréhéret, J.-G., 1997. L'Aptien et l'Albien de la fosse vocontienne (des bordures au bassin). Evolution de la sédimentation et enseignements sur les événements anoxiques. In: Société Géologique du Nord, Publication n° 25, p. 614.
Bréhéret, J.-G., Crumière, J.-P., 1989. Organic-rich episodes in the mid-Cretaceous (Aptian to Turonian) pelagic realm of the Vocontian Basin (SE France). Geobios, mémoire spécial 11, 205–210.
Caetano-Filho, S., Dias-Brito, D., Rodrigues, R., de Azevedo, R.L.M., 2017. Carbonate microfacies and chemostratigraphy of a late Aptian–early Albian marine distal section from the primitive South Atlantic (SE Brazilian continental margin): record of global ocean-climate changes? Cretac. Res. 74, 23–44.
Calvert, S.E., 1976. Chapter 33 - the mineralogy and geochemistry of near-shore sediments. In: Riley, J.P., Chester, R. (Eds.), Chemical Oceanography (Second Edition). Academic Press, pp. 187–280.
Coccioni, R., Erba, E., Premoli-Silva, I., 1992. Barremian-Aptian calcareous plankton biostratigraphy from the Gorgo Cerbara section (Marche, central Italy) and implications for plankton evolution. Cretac. Res. 13, 517–537.
Coccioni, R., Sabatino, N., Frontalini, F., Gardin, S., Sideri, M., Sprovieri, M., 2014. The neglected history of Oceanic Anoxic Event 1b: insights and new data from the Poggio le Guaine section (Umbria–Marche Basin). Stratigraphy 11, 245–282.
Corentin, P., Deconinck, J.-F., Pellenard, P., Amédro, F., Bruneau, L., Chenot, E., Matrion, B., Huret, E., Landrein, P., 2020. Environmental and climatic controls of the clay mineralogy of Albian deposits in the Paris and Vocontian basins (France). Cretac. Res. 108, 104342.
Cramer, B.S., Wright, J.D., Kent, D.V., Aubry, M.-P.C., 2003. Orbital climate forcing of δ13C excursions in the late Paleocene–early Eocene (chrons C24n–C25n). Paleoceanography 18, 1097.
Crowley, T.J., Kim, K.-Y., MEngel, J.G., Short, D.A., 1992. Modelling 100,000-year climate fluctuations in Pre-Pleistocene time series. Science 255, 705–707.
Erbacher, J., 1994. Entwicklung und Paläoozeanographie mittelkretazischer Radiolarien der westlichen Tethys (Italien) und des Nordatlantiks. Tübinger Mikropaläontogische Mitteilungen 12, 1–120.
Erbacher, J., Hemleben, C., Huber, B.T., Markey, M., 1999. Correlating environmental changes during early Albian oceanic anoxic event 1B using benthic foraminiferal paleoecology. Mar. Micropaleontol. 38, 7–28.
Erbacher, J., Huber, B.T., Norris, R.D., Markey, M., 2001. Increased thermohaline stratification as a possible cause for an ocean anoxic event in the Cretaceous period. Nature 409, 325–327.
Fantasia, A., Föllmi, K.B., Adatte, T., Spangenberg, J.E., Montero-Serrano, J.-C., 2018. The Early Toarcian oceanic anoxic event: paleoenvironmental and paleoclimatic change across the Alpine Tethys (Switzerland). Glob. Planet. Chang. 162, 53–68.
Ferry, S., 2017. Summary on Mesozoic carbonate deposits of the Vocontian Trough (Subalpine Chains, SE France). In: Granier, B. (Ed.), Some key Lower Cretaceous sites in Drôme (SE France), Carnets de Géologie, CG2017_B01.
Föllmi, K.B., 1996. The phosphorus cycle, phosphogenesis and marine phosphate-rich deposits. Earth Sci. Rev. 40, 55–124.
Föllmi, K.B., Bodin, S., Godet, A., Linder, P., Van de Schootbrugge, B., 2007. Unlocking paleo-environmental information from Early Cretaceous shelf sediments in the Helvetic Alps: stratigraphy is the key! Swiss J. Geosci. 100, 349–369.
Gale, A.S., Bown, P., Caron, M., Crampton, J., Crowhurst, S.J., Kennedy, W.J., Petrizzo, M.R., Wray, D.S., 2011. The uppermost Middle and Upper Albian succession at the Col de Palluel, Hautes-Alpes, France: an integrated study (ammonites, inoceramid bivalves, planktonic foraminifera, nannofossils, geochemistry, stable oxygen and carbon isotopes, cyclostratigraphy). Cretac. Res. 32, 59–130.
Gale, A.S., Mutterlose, J., Batenburg, S.J., 2020. The Cretaceous Period. In: Gradstein, F. M., Ogg, J.G., Schmitz, M.D., Ogg, G.M. (Eds.), Geologic Time Scale 2020, pp. 1023–1068.
Gavrilov, Y.O., Shcherbinina, E.A., Aleksandrova, G.N., 2019. Mesozoic and Early Cenozoic paleoecological events in the sedimentary record of the NE Peri-Tethys and adjacent areas: an overview. Lithol. Miner. Resour. 54 (6), 524–543.
Ghirardi, J., Deconinck, J.-F., Pellenard, P., Martinez, M., Bruneau, L., Amiotte-Suchet, P., Pucéat, E., 2014. Multi-proxy orbital chronology in the aftermath of the Aptian Oceanic Anoxic Event 1a: palaeoceanographic implications (Serre Chaitieu section, Vocontian Basin, SE France). Newsl. Stratigr. 47, 247–262.
Giorgioni, M., Weissert, H., Bernasconi, S.M., Hochuli, P.A., Coccioni, R., Keller, C.E., 2012. Orbital control on carbon cycle and oceanography in the mid-Cretaceous greenhouse. Paleoceanography 27, PA1204.
Giorgioni, M., Weissert, H., Bernasconi, S.M., Hochuli, P.A., Keller, C.E., Coccioni, R., Petrizzo, M.R., Lukeneder, A., Garcia, T.I., 2015. Paleoceanographic changes during the Albian-Cenomanian in the Tethys and North Atlantic and the onset of the Cretaceous chalk. Glob. Planet. Chang. 126, 46–61.
Gröcke, D., 2002. The carbon isotope composition of ancient CO_2 based on higher-plant organic matter. Philos. Trans. R. Soc. A Math. Phys. Eng. Sci. 360, 633–658.
Harper, D.T., Suarez, M.B., Uglesich, J., You, H., Li, D., Dodson, P., 2021. Aptian–Albian clumped isotopes from northwest China: cool temperatures, variable atmospheric pCO_2 and regional shifts in the hydrologic cycle. Clim. Past 17, 1607–1625.
Hay, W.W., DeConto, R.M., de Boer, P., Flögel, S., Song, Y., Stepashko, A., 2019. Possible solutions to several enigmas of Cretaceous climate. Int. J. Earth Sci. 108, 587–620.
Heimhofer, U., Hochuli, P.A., Burla, S., Andersen, N., Weissert, H., 2003. Terrestrial carbon-isotope records from coastal deposits (Algarve, Portugal): a tool for chemostratigraphic correlation on an intrabasinal and global scale. Terra Nova 15 (1), 8–13.
Herrle, J.O., Mutterlose, J., 2003. Calcareous nannofossils from the Aptian-Lower Albian of southeast France: palaeoecological and biostratigraphic implications. Cretac. Res. 24, 1–22.
Herrle, J.O., Pross, J., Friedrich, O., Kößler, P., Hemleben, C., 2003. Forcing mechanisms for mid-Cretaceous black shale formation: evidence from the Upper Aptian and Lower Albian of the Vocontian Basin (SE France). Palaeogeogr. Palaeoclimatol. Palaeoecol. 190, 399–426.
Herrle, J.O., Kössler, P., Friedrich, O., Erlenkeuser, H., Hemleben, C., 2004. High-resolution carbon isotope records of the Aptian to Lower Albian from SE France and the Mazagan Plateau (DSDP Site 545): a stratigraphic tool for paleoceanographic and paleobiologic reconstruction. Earth Planet. Sci. Lett. 218, 149–161.
Herrle, J.O., Schröder-Adams, C.J., Davis, W., Pugh, A.T., Galloway, J.M., Fath, J., 2015. Mid-Cretaceous High Arctic stratigraphy, climate, and Oceanic Anoxic Events. Geology 43, 403–406.
Holbourn, A., Kuhnt, W., Schulz, M., Flores, J.-A., Andersen, N., 2007. Orbitally-paced climate evolution during the middle Miocene "Monterey" carbon-isotope excursion. Earth Planet. Sci. Lett. 261, 534–550.
Huber, B.T., Leckie, R.M., 2011. Planktic foraminiferal species turnover across deep-sea Aptian/Albian boundary sections. J. Foraminifer. Res. 41, 53–95.
Huber, B.T., MacLeod, K.G., Watkins, D.K., Coffin, M.F., 2018. The rise and fall of the Cretaceous Hot Greenhouse climate. Glob. Planet. Chang. 167, 1–23.
Jenkyns, H.C., 1980. Cretaceous anoxic events: from continent to oceans. J. Geol. Soc. Lond. 137, 171–188.
Jenkyns, H.C., 2010. Geochemistry of oceanic anoxic events. Geochem. Geophys. Geosyst. 11 (Q03004), 1–30.
Joly, B., Delamette, M., 2008. Les Phylloceratoidea (Ammonoidea) aptiens et albiens du bassin vocontien (Sud-Est de la France). In: Notebooks on Geology, CG2008_M04, pp. 1–60.
Kennedy, J.W., Gale, A.S., Huber, B.T., Petrizzo, M.R., Bown, P., Jenkyns, H.C., 2017. The Global Boundary Stratotype Section and Point (GSSP) for the base of the Albian Stage, of the Cretaceous, the Col de Pré-Guittard section, Arnayon, Drôme, France. Episodes 40, 177–188.
Kuypers, M.M.M., Blokker, P., Erbacher, J., Kinkel, H., Pancost, R.D., Schouten, S., Damste, J.S.S., 2001. Massive expansion of marine archaea during a Mid-Cretaceous Oceanic Anoxic Event. Science 293, 92–94.
Kuypers, M.M.M., Pancost, R.D., Nijenhuis, I.A., Sinninghe Damsté, J.S., 2002. Enhanced productivity led to increased organic carbon burial in the euxinic North Atlantic basin during the late Cenomanian oceanic anoxic event. Paleoceanography 17, 1051.
Leckie, R.M., Bralower, T.J., Cashman, R., 2002. Oceanic anoxic events and plankton evolution: biotic response to tectonic forcing during the mid-Cretaceous. Paleoceanography 17 (3), 1–29.
Li, X., Wei, Y., Li, Y., Zhang, C., 2016. Carbon isotope records of the early Albian oceanic anoxic event (OAE) 1b from eastern Tethys (southern Tibet, China). Cretac. Res. 62, 109–121.
Ludvigson, G.A., Joeckel, R.M., Murphy, L.R., Stockli, D.F., González, L.A., Suarez, C.A., Kirkland, J.I., Al-Suwaidi, A., 2015. The emerging terrestrial record of Aptian-Albian global change. Cretac. Res. 56, 1–24.
Ma, W., Tian, J., Li, Q., Wang, P., 2011. Simulation of long eccentricity (400-kyr) cycle in ocean carbon reservoir during Miocene Climate Optimum: weathering and nutrient response to orbital change. Geophys. Res. Lett. 38, L10701.
MacQuaker, J.H.S., Keller, M.A., Davies, S.J., 2010. Algal blooms and "marine snow": mechanisms that enhance preservation of organic carbon in ancient fine-grained sediments. J. Sediment. Res. 80, 934–942.
Matsumoto, H., Kuroda, J., Coccioni, R., Frontalini, F., Sakai, S., Ogawa, N.O., Ohkouchi, N., 2020. Marine Os isotopic evidence for multiple volcanic episodes during Cretaceous Oceanic Anoxic Event 1b. Sci. Rep. 10, 12601.
Matsumoto, H., Shirai, K., Huber, B.T., MacLeod, K.G., Kuroda, J., 2023. High-resolution marine osmium and carbon isotopic record across the Aptian–Albian boundary in the southern South Atlantic: evidence for enhanced continental weathering and ocean acidification. Palaeogeogr. Palaeoclimatol. Palaeoecol. 613, 111414.
McAnena, A., Flögel, S., Hofmann, P., Herrle, J.O., Griesand, A., Pross, J., Talbot, H.M., Rethemeyer, J., Wallmann, K., Wagner, T., 2013. Atlantic cooling associated with a marine biotic crisis during the mid-Cretaceous period. Nat. Geosci. 6, 558–561.
Millán, M.I., Weissert, H.J., López-Horgue, M.A., 2014. Expression of the late Aptian cold snaps and the OAE1b in a highly subsiding carbonate platform (Aralar, northern Spain). Palaeogeogr. Palaeoclimatol. Palaeoecol. 411, 167–179.
Mort, H.P., Adatte, T., Föllmi, K.B., Keller, G., Steinmann, P., Matera, V., Berner, Z., Stüben, D., 2007a. Phosphorus and the roles of productivity and nutrient recycling during oceanic anoxic event 2. Geology 35, 483–486.
Mort, H.P., Jacquat, O., Adatte, T., Steinmann, P., Föllmi, K.B., Matera, V., Berner, Z., Stüben, D., 2007b. The Cenomanian/Turonian anoxic event at the Bonarelli Level in Italy and Spain: enhanced productivity and/or better preservation? Cretac. Res. 28, 597–612.
Mutterlose, J., Bornemann, A., Luppold, F.W., Owen, H.G., Ruffell, A., Weiss, W., Wray, D., 2003. The Vöhrum section (northwest Germany) and the Aptian/Albian boundary. Cretac. Res. 24, 203–252.

Navarro-Ramirez, J.-P., Bodin, S., Heimhofer, U., Immenhauser, A., 2015. Record of Albian to early Cenomanian environmental perturbation in the eastern sub-equatorial Pacific. Palaeogeogr. Palaeoclimatol. Palaeoecol. 423, 122–137.
O'Brien, C.L., Robinson, S.A., Pancost, R.D., Sinninghe Damsté, J.S., Schouten, S., Lunt, D.J., Alsenz, H., Bornemann, A., Bottini, C., Brassell, S.C., Farnsworth, A., Forster, A., Huber, B.T., Inglis, G.N., Jenkyns, H.C., Linnert, C., Littler, K., Markwick, P., McAnena, A., Mutterlose, J., Naafs, B.D.A., Püttmann, W., Sluijs, A., van Helmond, N.A.G.M., Vellekoop, J., Wagner, T., Wrobel, N.E., 2017. Cretaceous sea-surface temperature evolution: constraints from TEX86 and planktonic foraminiferal oxygen isotopes. Earth Sci. Rev. 172, 224–247.
Pälike, H., Norris, R.D., Herrle, J.O., Wilson, P.A., Coxall, H.K., Lear, C.H., Shackleton, N. J., Tripati, A.K., Wade, B.S., 2006. The heartbeat of the Oligocene climate system. Science 314, 1894–1898.
Pedersen, T.F., Clavert, S.E., 1990. Anoxia vs. productivity: what controls the formation of organic- carbon-rich sediments and sedimentary rocks? AAPG Bull. 74, 454–466.
Petrizzo, M.R., Huber, B.T., Gale, A.S., Barchetta, A., Jenkyns, H.C., 2012. Abrupt planktic foraminiferal turnover across the Niveau Kilian at Col de Pré-Guittard (Vocontian Basin, southeast France): new criteria for defining the Aptian/Albian boundary. Newslett. Stratigr. 45, 55–74.
Peybernes, C., Giraud, F., Jaillard, E., Robert, E., Masrour, M., Aoutem, M., Icame, N., 2013. Stratigraphic framework and calcareous nannofossil productivity of the Essaouira-Agadir Basin (Morocco) during the Aptian-Early Albian: comparison with the north-Tethyan margin. Cretac. Res. 39, 149–169.
Phelps, R.M., Kerans, C., Da-Gama, R.O.B.P., Jeremiah, J., Hull, D., Loucks, R.G., 2015. Response and recovery of the Comanche carbonate platform surrounding multiple Cretaceous oceanic anoxic events, northern Gulf of Mexico. Cretac. Res. 54, 117–144.
Price, G.D., 2003. New constraints upon isotope variation during the early Cretaceous (Barremian-Cenomanian) from the Pacific Ocean. Geol. Mag. 140, 513–522.
Riquier, L., Tribovillard, N., Averbuch, O., Devleeschouwer, X., Riboulleau, A., 2006. The Late Frasnian Kellwasser horizons of the Harz Mountains (Germany): two oxygen-deficient periods resulting from different mechanisms. Chem. Geol. 233, 137–155.
Robinson, S.A., Williams, T., Bown, P.R., 2004. Fluctuations in biosiliceous production and the generation of Early Cretaceous oceanic anoxic events in the Pacific Ocean (Shatsky Rise, Ocean Drilling Program Leg 198). Paleoceanography 19, PA4024.
Sabatino, N., Coccioni, R., Salvagio Manta, D., Baudin, F., Vallefuoco, M., Traina, A., Sprovieri, M., 2015. High-resolution chemostratigraphy of the late Aptian-early Albian oceanic anoxic event (OAE 1b) from the Poggio le Guaine section (Umbria-Marche Basin, central Italy). Palaeogeogr. Palaeoclimatol. Palaeoecol. 426, 319–333.
Sabatino, N., Ferraro, S., Coccioni, R., Bonsignore, M., Del Core, M., Tancredi, V., Sprovieri, M., 2018. Mercury anomalies in upper Aptian-lower Albian sediments from the Tethys realm. Palaeogeogr. Palaeoclimatol. Palaeoecol. 495, 163–170.
Schlanger, S.O., Jenkyns, H.C., 1976. Cretaceous oceanic anoxic events: causes and consequences. Geol. Mijnb. 55, 179–184.
Scotese, C.R., 2016. PALEOMAP PaleoAtlas for GPlates and the PaleoData Plotter Program. http://www.earthbyte.org/paleomap-paleoatlas-for-gplates/(2016).
Sinninghe Damsté, J.S., Kok, M.D., Köster, J., Schouten, S., 1998. Sulfurized carbohydrates: an important sedimentary sink for organic carbon? Earth Planet. Sci. Lett. 164, 7–13.
Sluijs, A., Dickens, G.R., 2012. Assessing offsets between the $\delta^{13}C$ of sedimentary components and the global exogenic carbon pool across early Paleogene carbon cycle perturbations. Glob. Biogeochem. Cycles 26, GB4005.
Stein, M., Föllmi, K.B., Westermann, S., Godet, A., Adatte, T., Matera, V., Fleitmann, D., Berner, Z., 2011. Progressive palaeoenvironmental change during the Late Barremian-Early Aptian as prelude to Oceanic Anoxic Event 1a: evidence from the Gorgo a Cerbara section (Umbria-Marche basin, central Italy). Palaeogeogr. Palaeoclimatol. Palaeoecol. 302, 396–406.
Storm, M.S., Hesselbo, S.P., Jenkyns, H.C., Ruhl, M., Ullmann, C.V., Xu, W., Leng, M.J., Riding, J.B., Gorbanenko, O., 2020. Orbital pacing and secular evolution of the Early Jurassic carbon cycle. Proc. Natl. Acad. Sci. 117, 3974–3982.
Strasser, A., Caron, M., Gjermeni, M., 2001. The Aptian, Albian and Cenomanian of Roter Sattel, Romandes Prealps, Switzerland: a high-resolution record of oceanographic changes. Cretac. Res. 22 (2), 173–199.
Suan, G., van de Schootbrugge, B., Adatte, T., Fiebig, J., Oschmann, W., 2015. Calibrating the magnitude of the Toarcian carbon cycle perturbation. Paleoceanography 30, PA002758.
Suarez, M.B., Milder, T., Peng, N., Suarez, C.A., You, H., Li, D., Dodson, P., 2018. Chemostratigraphy of the Lower Cretaceous dinosaur-bearing Xiagou and Zhonggou formations, Yujingzi Basin, northwest China. J. Vertebr. Paleontol. 38, 12–21.
Tessin, A., Hendy, I.L., Sheldon, N.D., Sageman, B.C.P.A., 2015. Redox-controlled preservation of organic matter during "OAE 3" within the Western Interior Seaway. Paleoceanography 30, 702–717.
Trabucho Alexandre, J., van Gilst, R.I., Rodríguez-López, J.P., De Boer, P.L., 2011. The sedimentary expression of oceanic anoxic event 1b in the North Atlantic. Sedimentology 58, 1217–1246.
Tyrrell, T., 1999. The relative influences of nitrogen and phosphorus on oceanic primary production. Nature 400, 525–531.
Tyson, R.V., 2005. The "productivity versus preservation" controversy: cause, flaws, and resolution. In: Harris, N.B. (Ed.), Deposition of Organic-Carbon-Rich Sediments: Models, SEPM Special Publication, 82, pp. 17–33.
Ullmann, C.V., Boyle, R., Duarte, L.V., Hesselbo, S.P., Kasemann, S.A., Klein, T., Lenton, T.M., Piazza, V., Aberhan, M., 2020. Warm afterglow from the Toarcian Oceanic Anoxic Event drives the success of deep-adapted brachiopods. Sci. Rep. 10, 6549.
Voigt, S., Aurag, A., Leis, F., Kaplan, U., 2007. Late Cenomanian to Middle Turonian high-resolution carbon isotope stratigraphy: new data from the Münsterland Cretaceous Basin, Germany. Earth Planet. Sci. Lett. 253, 196–210.
Wagner, T., Wallmann, K., Herrle, J.O., Hofmann, P., Stuesser, I., 2007. Consequences of moderate ~25,000 yr lasting emission of light CO2 into the mid-Cretaceous ocean. Earth Planet. Sci. Lett. 259, 200–211.
Wagner, T., Herrle, J.O., Sinninghe Damsté, J.S., Schouten, S., Stüsser, I., Hofmann, P., 2008. Rapid warming and salinity changes of Cretacous surface waters in the subtropical North Atlantic. Geology 36, 203–206.
Wang, Y., Bodin, S., Blusztajn, J.S., Ullmann, C.V., Nielsen, S.G., 2022. Orbitally-paced global oceanic deoxygenation decoupled from volcanic CO2 emission during the middle Cretaceous OAE 1b (Aptian-Albian transition). Geology 50, 1324–1328.
Wei, W., Algeo, T.J., 2020. Secular variation in the elemental composition of marine shales since 840 Ma: tectonic and seawater influences. Geochim. Cosmochim. Acta 287, 367–390.
Xu, X., Shao, L., Eriksson, K.A., Zhou, J., Wang, D., Hou, H., Hilton, J., Wang, S., Lu, J., Jones, T.P., 2022. Widespread wildfires linked to early Albian Ocean Anoxic Event 1b: evidence from the Fuxin lacustrine basin, NE China. Global Planet. Change 215, 103858.
Zachos, J.C., McCarren, H., Murphy, B., Röhl, U., Westerhold, T., 2010. Tempo and scale of late Paleocene and early Eocene carbon isotope cycles: Implications for the origin of hyperthermals. Earth Planet. Sci. Lett. 299, 242–249.